THE UNIVERSITY OF QUEENSLAND

AUSTRALIA

Differential Diffusion in Multiple Mapping Conditioning (MMC) Model

Leila Dialameh

Master of Mechanical Engineering

A thesis submitted for the degree of Master of Philosophy at

The University of Queensland in 2018

School of Mechanical and Mining Engineering

Abstract

This thesis describes the recent development in the Multiple Mapping Conditioning (MMC) method for non-premixed turbulent combustion focussing on differential diffusion effects. Turbulent combustion is a considerable issue in different engineering fields during the last decades. Nowadays, there are more global concerns on sustainability, environmental impacts and efficiency of fuels. These challenges have motivated additional research to maximize the efficiency and reduce pollutants of future combustion systems.

Modelling of turbulent combustion is a complementary approach to experimental analysis of combustors. In general, mixture-fraction based methods and joint Probability Distribution Function (PDF) methods are two main categories for turbulent combustion modelling. MMC, which is the subject of this thesis, combines the useful features of the two aforementioned categories and is applicable to both premixed and non-premixed combustion. One of the great advantages of MMC is localising mixing within an independent *reference space*, which enforces localness of mixing in the composition space.

Differential diffusion effects due to differences in molecular diffusivity of species are neglected in most turbulent combustion models for simplification. However for the cases of fuels containing highly diffusive species (e.g. hydrogen), ignoring these effects leads to errors evidenced by many experimental and numerical works in literature. Hydrogen and hydrogen-enriched fuels are of interest as an alternative to fossil fuels, which can address environmental concerns. Therefore, combustion models need to be improved to include differential diffusion.

In the present thesis, two MMC models are suggested and implemented for emulating differential diffusion effects in a homogeneous turbulent non-reacting flow. A *side stepping* approach is developed to obtain benefits of MMC in conjunction with and theoretical analysis of differential diffusing scaling of physical parameters of flow. This approach accounts for differential decay rate of scalar variances, which is one of the key effects of differential diffusion. It is shown that this novel MMC model can also emulate the decorrelation of scalars, which is a more refined differential diffusion effect. Results indicate good agreement with the previous DNS studies.

Declaration by author

This thesis is composed of my original work, and contains no material previously published or written by another person except where due reference has been made in the text. I have clearly stated the contribution by others to jointly-authored works that I have included in my thesis.

I have clearly stated the contribution of others to my thesis as a whole, including statistical assistance, survey design, data analysis, significant technical procedures, professional editorial advice, financial support and any other original research work used or reported in my thesis. The content of my thesis is the result of work I have carried out since the commencement of my higher degree by research candidature and does not include a substantial part of work that has been submitted to qualify for the award of any other degree or diploma in any university or other tertiary institution. I have clearly stated which parts of my thesis, if any, have been submitted to qualify for another award.

I acknowledge that an electronic copy of my thesis must be lodged with the University Library and, subject to the policy and procedures of The University of Queensland, the thesis be made available for research and study in accordance with the Copyright Act 1968 unless a period of embargo has been approved by the Dean of the Graduate School.

I acknowledge that copyright of all material contained in my thesis resides with the copyright holder(s) of that material. Where appropriate I have obtained copyright permission from the copyright holder to reproduce material in this thesis and have sought permission from co-authors for any jointly authored works included in the thesis.

Publications included in this thesis

-Incorporated as chapter 4

Dialameh, L., Cleary, M. J. and Klimenko, A. Y. (2014) A multiple mapping conditioning model for differential diffusion. Physics of Fluids, 26 2: doi:10.1063/1.4864101

Contributor	Statement of contribution
L. Dialameh (Candidate)	Developed method (60%) Wrote code and ran simulations (80%) Analysed results (60%) Wrote and edited paper (60%)
A. Y. Klimenko	Developed method (30%) Wrote code and ran simulations (20%) Analysed results (20%) Wrote and edited paper (10%)
M. J. Cleary	Developed method (10%) Analysed results (20%) Wrote and edited paper (30%)

Submitted manuscripts included in this thesis

No manuscripts submitted for publication.

Other publications during candidature

Conference papers:

Dialameh, L., Sundaram, B., Cleary, M. J. and Klimenko, A. Y. (2012). Differential diffusion of passive scalars with MMC mixing model in isotropic turbulent flow. In: P. A. Brandner and B. W. Pearce, Proceedings of the 18th Australasian Fluid Mechanics Conference. 18th Australasian Fluid Mechanics Conference (AFMC), Launceston, Australia, 3-7 December 2012.

Sundaram, Brruntha, Dialameh, Leila, Cleary, Matthew, Klimenko, A. Y. and Ge, Yipeng (2013). Multiple mapping conditioning: the concept and its development. In: ECM 2013: 6th European Combustion Meeting 2013, Lund, Sweden, 25-28 June, 2013.

Dialameh, L., Sundaram, B., Ge, Y., Cleary, M. J. and Klimenko, A. Y. (2013). Recent developments of the multiple mapping conditioning mixing model. In: ICDERS 2013: 24th International Colloquium on the Dynamics of Explosions and Reactive Systems, Taipei, Taiwan, 28 July-2 August, 2013.

Dialameh, L., Cleary, M. J. and Klimenko, A. Y. (2013). Differential diffusion effects in Multiple Mapping Conditioning (MMC) mixing model. In: Mingming Zhu, Yu Ma, Yun Yu, Hari Vuthaluru, Zhezi Zhang and Dongke Zhang, Australian Combustion Symposium 2013: Proceedings. ACS2013: Australian Combustion Symposium 2013, Crawley, WA, Australia, (158-161). 6-8 November, 2013.

Contributions by others to the thesis

No contributions by others.

Statement of parts of the thesis submitted to qualify for the award of another degree

No works submitted towards another degree have been included in this thesis.

Research Involving Human or Animal Subjects

No animal or human subjects were involved in this research.

Acknowledgements

I would like to express my deep gratitude to my supervisors Dr Alexander Klimenko and Dr Matthew Cleary, who supported and guided me during my study. The achievement of this thesis would not have been possible without their assistance and constructive advices.

I would like to thank Dr. Brruntha Sundaram for all her help during my study.

My gratitude goes to my parents, my beautiful daughter, Dornika, and my best husband, Mojtaba, who supported me through this journey.

I also acknowledge the financial support of the Australian Research Council and the Australian Post Graduate Award as well as kind support of staff in the School of Mechanical and Mining Engineering.

Financial support

This research was supported by an Australian Research Council and the Australian Post Graduate Award.

Keywords

turbulent combustion, Multiple Mapping Conditioning, MMC, differential diffusion, non-premixed

Australian and New Zealand Standard Research Classifications (ANZSRC)

ANZSRC code: 091508 Turbulent Flows, 100%

Fields of Research (FoR) Classification

FoR code: 0915 Interdisciplinary Engineering, 100%

Table of Contents

List of Figures

List of Tables

Chapter 1 - Introduction

Combustion is a major class of reactions, in which chemical energy is converted to heat due to a sequence of reactions involving a fuel and an oxidiser. Combustion is very important for a broad range of residential, commercial and industrial uses such as power generation, transportation, manufacturing, heating and cooling systems of buildings and even cooking.

Fossil fuels are still the main source of energy, supplying more than 80% of the world's demands in 2015 [1]. Depletion of fossil fuels due to rapid increase in their consumption raises concerns on energy security and the extent of reserves. Moreover, the environmental impact of fossil fuels and their huge contribution to global warming effects are under increasing scrutiny. An unavoidable by-product of burning hydrocarbon fuels is carbon dioxide (CO_2), which is the gas responsible for exacerbating greenhouse effects High concentrations of CO_2 in the atmosphere lead to increases in global average temperature [2]. Other pollutants of hydrocarbon combustion are carbon monoxide (CO), nitrous oxides (NOx), sulphur oxides (SOx) and soot. Therefore, fossil fuels consumption is linked to air pollution, climate change and energy security.

These issues may be addressed in several ways. Firstly, a switch to renewable energy sources like solar and wind or nuclear energy may be chosen. Secondly, other alternatives to fossil fuels like biofuels and hydrogen may be used. Biofuels are any kinds of solid, liquid or gaseous fuels derived from biomass. Examples of biofuels include vegetable oil, biodiesel, bio-alcohols, biogas, solid biofuels and syngas [3]. Hydrogen is another attractive alternative to fossil fuels which has motivated recent research (e.g. [4],[5], [6],[7],[8],[9]). The main advantages of hydrogen are that it burns easily and can be used almost directly in well-developed systems. More importantly, burning hydrogen eliminates hydrocarbon emission, which is a big challenge of current decade. The final feasible way is to improve methods for emissions control of hydrocarbon fuels. These methods can be divided to the pre-processing of fuels, the post-treatment of exhaust gases and the modification of the combustion process.

All the aforementioned challenges in combustion technology are evidence of the vitality of new research and development in this area. Turbulent combustion flow is complicated to predict due to the complexity of coupled interactions between chemistry and turbulence as well as its multiscale nature. Considerable contribution and investment are essential for

both advanced model improvement approaches as well as high quality experimental studies to provide a depth of physical insights and basis for model validation.

Turbulent combustion modelling approaches belong either exclusively, or as a combination of two main categories as follow. The first one is mixture fraction based methods such as Fast chemistry by Bilger [10] , the Flamelet model of Peters [11] , [12] and the Conditional Moment Closure (CMC) model of Klimenko and Bilger [13]. The second category is Probability Density Function (PDF) method of Pope [14] , [15]. The main advantage of PDF methods is the closure of the chemical source term, although the conditional scalar dissipation term is still unclosed and needs to be modelled by a mixing operation.

The Multiple Mapping Conditioning (MMC) model of Klimenko and Pope [16] is a relatively recent approach that effectively combines the useful and beneficial features of two above mentioned categories. MMC is the subject of this study and is explained in further detail in Chapter 2.

Most turbulent combustion models, however, have limited predictive capabilities in some practical applications. One of the deficiencies is the neglect of differential diffusion or the difference in molecular diffusivity of various chemical species. Differential diffusion is neglected in many models because it is assumed that turbulent mixing is dominant over molecular mixing, leading to great model simplifications. However, there are numerous experimental and numerical DNS studies in the literature that indicate the importance of differential diffusion effects especially in flows with specifically low or highly diffusive species.

One of the most important thermo-physical properties of hydrogen is its high diffusivity relative to other gases. Therefore, considering differential diffusion is essential for accurate combustion predictions of hydrogen and hydrogen-rich fuels. This leads to the motivation of this work to improve turbulent combustion models to predict differential diffusion effects.

It is the objective of this thesis to advance the development of the Multiple Mapping Conditioning (MMC) method to include differential diffusion effects.

The remainder of this thesis is organised as follows.

Chapter 2 contains a brief review of different scales of turbulent motions followed by governing equations and numerical methods of turbulent combustion. Different turbulent combustion models for non-premixed combustion, which is the combustion category in this

research, are discussed with particular attention devoted to the Multiple Mapping Conditioning (MMC) model. Deterministic, stochastic and generalised versions of MMC are addressed briefly.

In Chapter 3, the literature and physics of differential diffusion are discussed. Numerical and experimental studies as well as different turbulent combustion model developments for differential diffusion are reviewed.

In Chapter 4 differential diffusion of unreactive, passive scalars in statistically stationary, isotropic turbulent flow is studied. In the first part, the Reynolds and Schmidt number scaling of differential diffusion is theoretically developed and compared with available results in literature. This is achieved by in-depth analysis of the energy and variance spectrum of two passive scalars in wide range of wavenumber band. In the second part, two improved MMC models for differential diffusion are suggested and implemented: i) a one reference variable model and ii) a two reference variable model. The ability of these models to account for differential diffusion effects are demonstrated and successfully validated against DNS results of Yeung and Pope [17] and Yeung and Luo [18].

The overall conclusions and discussion are presented in Chapter 5.

Chapter 2 - Fundamentals of turbulent combustion modelling

Literature relevant to this thesis is presented in this chapter. First, an overview of different scales of turbulent motion is discussed. This is followed by conservation equations, which govern turbulent combustion flows as well as the numerical methods to solve them. Then the concept of non-premixed combustion, which is considered in this research, is addressed. Different turbulent combustion modelling approaches are discussed briefly with more details on Multiple Mapping Conditioning, MMC, model that is the subject of this study.

2.1. The scale of turbulent motion

Turbulence generally occurs when laminar flows become unstable at a critical Reynolds number. The Reynolds number, Re, is defined as the ratio of advection (inertia) to diffusion (viscous) force:

$$\mathrm{Re} = \frac{uL}{\nu} \qquad (2.1)$$

where L is a characteristic length scale, u is a characteristic velocity and ν is the kinematic viscosity of the fluid.

The first concept of Richardson's [19] energy cascade is the occurrence of eddies of different length scales in turbulent flow. "In brief, the idea of energy cascade is that kinetic energy enters the turbulence through the production mechanism at the largest scales of the motion. This energy is then transferred by inviscid processes to smaller and smaller scales until at the smallest scales, the energy is dissipated by viscous action." [15] . The four scales, in decreasing order of size, are: macroscale, L, integral scale, l_0, Taylor microscale, λ, and Kolmogorov microscale, η.

The most accepted theory of turbulence is based on the *energy cascade* concept developed by Kolmogorov [20]. It is based on three important hypotheses:

- *Kolmogorov's hypothesis of local isotropy*- at sufficiently high Reynolds numbers, the small-scale turbulent motions ($l \ll l_0$) are statistically isotropic.

- *Kolmogorov's first similarity hypothesis* **-** in every turbulent flow at sufficiently high Reynolds number, the statistics of the small scale motions have a universal form that is uniquely determined by the dissipation rate , ε , and the kinematic viscosity , ν .
- *Kolmogorov's second similarity hypothesis***-** in every turbulent flow at sufficiently high Reynolds number, the statistics of the motions of scale l in the range $l_0 \gg l \gg \eta$ have a universal form that is uniquely determined by ε independent of ν [15].

Figure 2.1 illustrates the energy cascade at high Reynolds number. The subscripts EI and DI indicate that l_{EI} is the demarcation line between energy , E , and inertial , I , ranges, as l_{DI} is between the dissipation , D , and inertial , I , ranges [15].

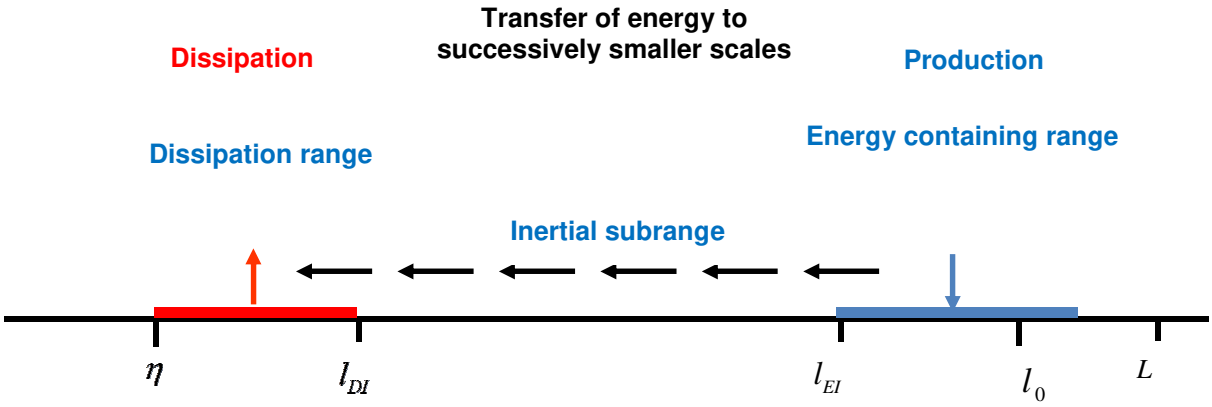

Figure 2.1. A schematic diagram of the energy cascade at high Reynolds number [15]

The second similarity hypothesis of Kolmogorov leads to the well- known $k^{-5/3}$ law for the kinetic energy spectrum, $E(k)$, and variance spectrum of a passive scalar, $E_\theta(k)$, in the inertial subrange. These spectral regimes of the kinetic energy and scalar variance are found in wavenumber bands determined by the integral scales of turbulence and three dissipation scales depend on the Schmidt number.

The Schmidt number, Sc , is defined as

$$Sc = \frac{\nu}{D} \qquad (2.2)$$

where ν is the kinematic viscosity and D is the molecular diffusivity.

The above mentioned dissipation length scales and their corresponding wavenumbers are as follow:

The Kolmogorov scale: $$k_K = \left(\frac{\varepsilon}{\nu^3}\right)^{1/4} = \frac{1}{\eta} \qquad (2.3)$$

The Batchelor scale : $$k_B = \left(\frac{\varepsilon}{\nu D^2}\right)^{1/4} = k_K Sc^{1/2} = \frac{1}{\eta_B} \qquad (2.4)$$

The Obukhov-Corrsin scale $$k_{OC} = \left(\frac{\varepsilon}{D^3}\right)^{1/4} = k_K Sc^{3/4} = \frac{1}{\eta_{OC}} \qquad (2.5)$$

Based on Kolmogorov's eddy cascade hypothesis, in the inertial subrange, $\frac{1}{k} < l < \frac{1}{\eta}$, the kinetic energy spectrum scaled as

$$E(k) = C_k \varepsilon^{2/3} k^{-5/3} \qquad (2.6)$$

where C_k is a universal Kolmogorov constant. Figure 2.2 represents the turbulent energy spectrum in the entire ranges as a function of wavenumber in log-log plot.

As can be seen in Figure 2.2, for small wavenumbers the energy per unit wavenumber increases with a power law between k^2 and. k^4. The spectrum reaches a maximum value at the integral scale wavenumber. In the inertial subrange or larger wavenumbers, the energy spectrum decreases following the $k^{-5/3}$ law. At the Kolmogorov scale there is a cutoff while in the viscous subrange the energy decreases exponentially due to viscous effects.

A similar hypothesis predicts that the variance spectrum of a passive scalar, $E_\theta(k)$, also has a $k^{-5/3}$ inertial–convective regime [21, 22]. The inertial-convective subrange of the scalar-variance spectrum for the wavenumbers below the Obukhov-Corrsin, scaled as

$$E_\theta(k) = C_\theta \chi \varepsilon^{-1/3} k^{-5/3} \qquad (2.7)$$

where C_θ is the Obukhov-Corrsin constant.

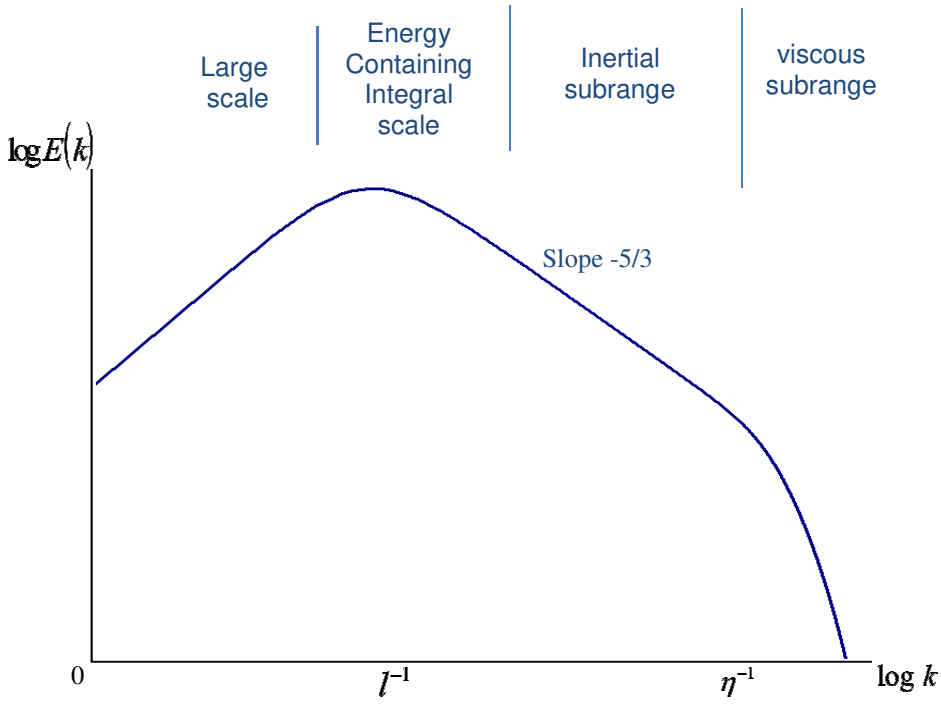

Figure 2.2. Turbulent kinetic energy spectrum as a function of the wavenumber [12]

Batchelor [23] predicted that the variance spectrum between the inertial-convective subrange and the scalar-dissipation regime is determined by the Schmidt number and the ordering of the wavenumber cutoffs.

Two cases are considered:

I. High Schmidt number ,$\nu \gg D$

In this case the wavenumber cutoffs are ordered as $k_k < k_B < k_{OC}$ and the scalar variance dissipates at the Batchelor scale while the turbulent kinetic energy dissipates at the

Kolmogorov microscale. Moreover, the inertial-convective subrange is more extensive than the inertial subrange [24]. Batchelor [23] predicted the viscous-convective spectrum in this range as follow

$$E_\theta(k) = q\chi\left(\frac{\nu}{\varepsilon}\right)^{1/2} k^{-1} \qquad (2.8)$$

where q is the Batchelor constant.

Figure 2.3 illustrates spectra of variance and energy for this case in log-log plot. As can be seen, for the case of high Schmidt number the scalar variance dissipates at the Batchelor scale while the turbulent kinetic energy dissipates at the Kolmogorov scale.

II. Low Schmidt number , $\nu \ll D$

For this case the wavenumber cutoffs are ordered as these are ordered as $k_{OC} < k_k$ and the scalar variance dissipates at Obukhov-Corrsin scale while the turbulent kinetic energy dissipates at the Kolmogorov microscale. Figure 2.4 shows log-log plot of the $E_\theta(k)$ and $E(k)$ for case II.

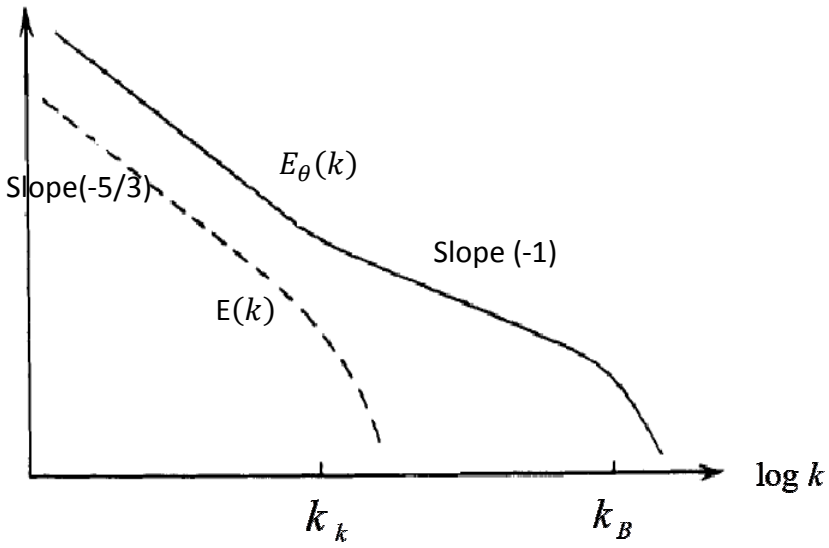

Figure 2.3. Energy and variance spectrum for case I- high Schmidt number

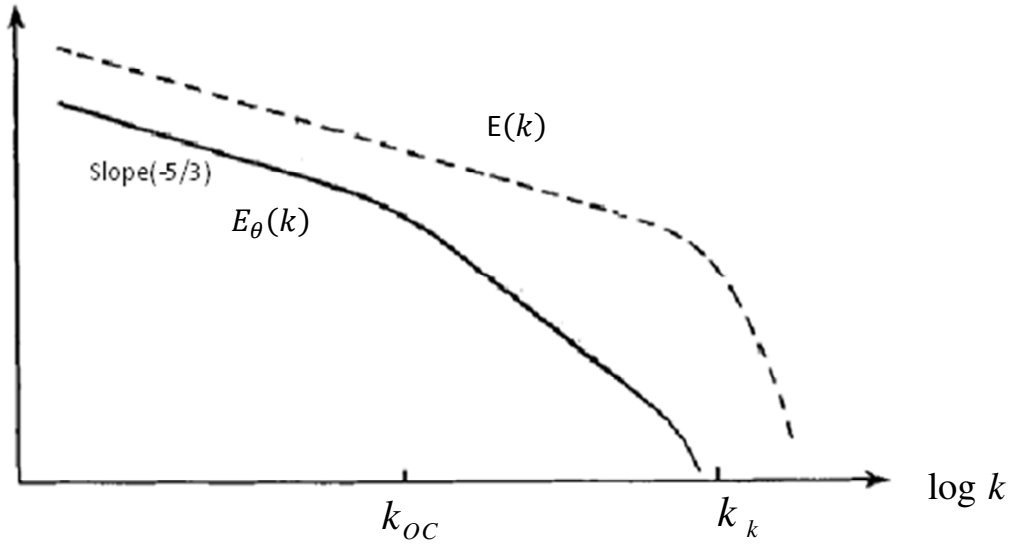

Figure 2.4. Energy and variance spectrum for case II- low Schmidt number

2.2. Conservation equations

The numerical modeling of turbulent combustion problems is based on the solution of a set of conservation equations for momentum and scalars, plus additional auxiliary equations such as state equations. These equations for reacting ,ideal gas mixtures are summarized below [25]. In the following equations, ∇ is the gradient operator, U is the unit tensor, two dots $(:)$ indicate that the tensors are to be contracted twice and the superscript T denotes the transpose of the vector. Simplifying assumptions can be made for following described set of equations.

- **Continuity**

The continuity equation states that mass can be transported by convection but cannot be created or destroyed. As the flow is reacting, density changes and the continuity equation cannot be simplified

$$\frac{\partial \rho}{\partial t} + \nabla \cdot (\rho \vec{V}) = 0 \qquad (2.9)$$

where ρ is density and $\vec{V}$ is the mass average-velocity vector of the gas mixture.

- **Momentum**

The momentum conservation, equation accounts for external and internal forces which act on a control volume of fluid, is as follow

$$\frac{\partial \vec{V}}{\partial t} + \vec{V} \cdot \vec{\nabla} V = -(\nabla \cdot \vec{P}) / \rho + \sum_{i=1}^{N} Y_i \vec{f}_i \qquad (2.10)$$

where $\vec{f}_i$ is the external force per unit mass on species i and $\vec{P}$ is the stress tensor defined as follow

$$\vec{P} = \left[p + \left(\frac{2}{3}\mu - k \right)(\nabla \cdot \vec{V}) \right] \vec{U} - \mu[(\nabla \vec{V}) + (\nabla \vec{V})^T] \qquad (2.11)$$

and p is hydrostatic pressure, μ is the coefficient of shear viscosity and k is the bulk viscosity coefficient.

- **Conservation of species**

  For $i = 1, ..., N$

$$\frac{\partial Y_i}{\partial t} + \vec{V} \cdot \nabla Y_i = w_i / \rho - [\partial \cdot (\rho Y_i V_i)] / \rho \qquad (2.12)$$

where V_i is the diffusion velocity of species i , Y_i is mass fraction of species i and w_i is the reaction rate which defines in equation (2.15).

- **Energy**

Conservation of energy is given by

$$\rho \frac{\partial u}{\partial t} + \rho \vec{v} \cdot \nabla u = -\nabla \cdot \vec{q} - \vec{P} : (\nabla \vec{v}) + \rho \sum_{i=1}^{N} Y_i \vec{f}_i \cdot V_i \qquad (2.13)$$

where u is the intenal energy per unit mass for the mixture and $\vec{q}$ is the heat flux vector which is defined as

$$\vec{q} = -\lambda \nabla T + \rho \sum_{i=1}^{N} h_i Y_i \vec{V}_i + R^0 T \sum_{i=1}^{N} \sum_{j=1}^{N} \left(\frac{X_j D_{T,i}}{W_i D_{i,j}} \right) (\vec{V}_i - \vec{V}_j) + \vec{q}_R \qquad (2.14)$$

where λ is thermal conductivity , h_i is specific enthalpy of species i , R^0 is universal gas constant, X_i is mole fraction of species i , W_i is molecular weight of species i , $D_{T,i}$ is thermal diffusion coefficient for species i, $D_{i,j}$ is binary diffusion coefficient and. $\vec{q}_R$ is the radiant heat flux vector.

- **Chemical reaction rate**

The chemical reaction rate, w_i, from equation (2.12) can be determined through chemical kinetics for M number of reactions and a combination of simpler expressions for the reaction rate, law of mass action and forward and reverse reaction rate constants as follow

For $j = 1,...,N$

$$w_i = W_i \sum_{k=1}^{M} (v_{i,k}^{''} - v_{i,k}^{'}) B_k T^{\alpha_k} e^{-(E_k / R^0 T)} \prod_{j=1}^{N} \left(\frac{X_j p}{R^0 T} \right) \qquad (2.15)$$

where. W_i is molecular weight of species i, $v_{i,k}^{'}$ and $v_{i,k}^{''}$ are the stoichiometric coefficients for species i appearing as reactant and product respectively in reaction k. B_k is a constant in the frequency factor for the k th reaction and α_k is the exponent determining the temperature dependence of the frequency factor for the k th reaction and E_k .is activation energy for the k th reaction.

- **State equations**

State equations enable to evaluate thermodynamics properties from known properties .A common relation involves the ideal gas law are as follow

For $i = 1,...,N$

The hydrostatic pressure:

$$p = \rho R^0 T \sum_{i=1}^{N} \left(Y_i \Big/ W_i \right) \qquad (2.16)$$

The internal energy per unit mass for the gas mixture:

$$u = \sum_{i=1}^{N} h_i Y_i - p/\rho \qquad (2.17)$$

The specific enthalpy of species i:

$$h_i = h_i^0 + \int_{T^0}^{T} c_{p,i} dT \qquad (2.18)$$

The mole fraction of species i :

$$X_i = \frac{Y_i / W_i}{\sum_{j=1}^{N} (Y_j / W_j)} \qquad (2.19)$$

2.3. Computational approaches for turbulent combustion

In Computational Fluid Dynamics, the solution of turbulent combustion can be achieved at three different levels. The highest level of simulation is Direct Numerical Simulation (DNS) where the full instantaneous Navier-Stokes equations are solved with no model requirements for turbulent motions. It is necessary to use minor time step and very fine mesh in this level. As a result, resolving the entire spectrum needs large number of grid points proportional to Reynolds number cubed, Re^3.

Large Eddy Simulation (LES) is the second level simulation approaches for solving the Navier-Stokes equations. In LES the turbulent large scales are calculated explicitly while the effects of smaller scales are modelled using sub grid closure models. Filtering is the main concept of LES that consider which scales to keep and which scales to discard.

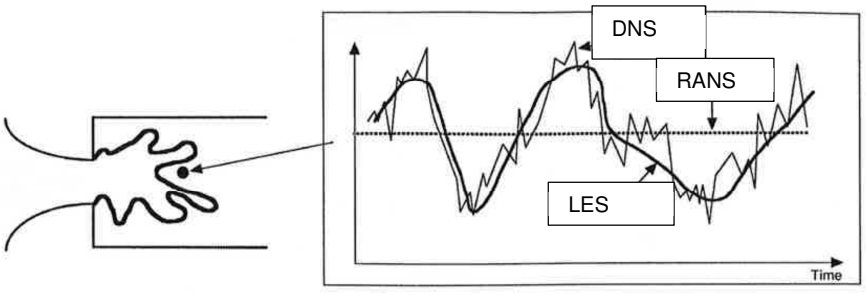

Figure 2.5 Time evolution of local temperature in a turbulent flame computed with DNS, RANS and LES [26]

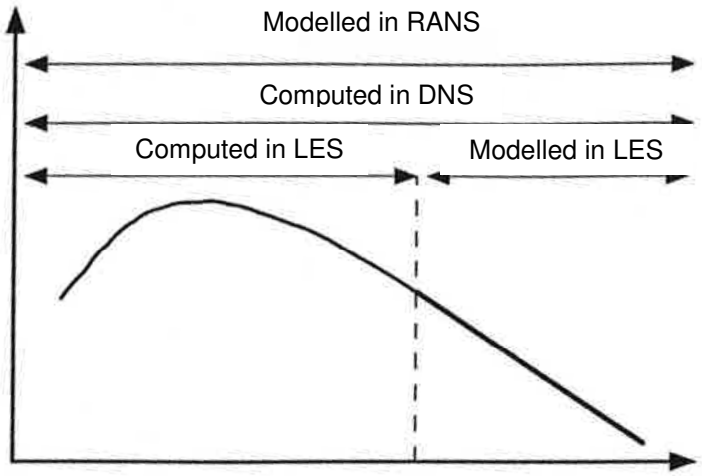

Figure 2.6 Turbulent Energy spectrum as a function of wave number [26]

Table 2.1 Comparison between RANS, LES and DNS [26]

Approach	Advantages	Drawbacks
RANS	• coarse numerical grid • geometrical simplification (2D flows, symmetry,...) • reduced numerical costs	• only mean flow field • models required
LES	• unsteady features • reduced modelling impact (compared to RANS)	• models required • 3D simulations required • needs precise codes • numerical costs
DNS	• no models needed for turbulence/ combustion interaction • tool to study models	• prohibitive numerical costs(fine grids, precise codes) • limited to academic problems

Reynolds Averaged Navier Stokes (RANS) is the most computationally efficient solving model for combustion simulation, which only solves the mean value for all quantities.

RANS, LES and DNS models are summarised [26] in terms of frequency and energy spectrum in Figures 2.5 and 2.6 respectively. All frequencies in the spectrum are resolved in DNS while only the largest scales up to a cut-off wave number are computed in LES and the effects of the smaller motions are modelled. In RANS, only the mean flow fields are resolved.

Comparisons between RANS, LES and DNS are briefly summarised in Table 2. 1 [26].

2.4. Turbulent non-premixed combustion

The combustion categories are divided into premixed and non-premixed. In non-premixed combustion, the reactants, fuel and oxidizer, enter separately into the combustor where mixed and burnt. In premixed combustion, reactants are completely mixed before combustion takes place.

Many combustors operate in the non-premixed mode, often for safety reasons and elimination of the risk of explosion. Moreover, non-premixed burners are relatively simpler to design. Gas turbine, diesel engines; boilers, furnaces, chemical lasers and rocket exhaust plumes are some examples of non-premixed flows.

A very important dimensionless number associated with the non-premixed flames is known as the Damköhler number, Da. It is defined as the ratio of the mixing phenomena time scale that is the time required for both convection and diffusion in the system to the chemical reaction time scale. There are two categories of turbulent non-premixed combustion models based on Da number: i) infinite-rate chemistry or fast chemistry and ii) finite-rate chemistry.

In infinite-rate chemistry, the chemical reactions are much faster than the other processes so the chemical time is typically smaller than mixing time and the Da number is large. Moreover, the flame can be consider as a laminar flame while the chemical reactions are irreversible [12]. The elimination of all finite rate chemical kinetics parameters introduces important simplifications while the fast chemistry assumption is valid.

In some situations where diffusion time scales are not so large in comparison to the chemical reaction times, the fast chemistry assumption is invalid and unsteady effects

should be considered. This case is known as finite rate chemistry that is typically associated with low Da numbers.

Table 2.2 Summary of turbulent combustion models in non-premixed combustion [12]

Infinitely fast chemistry	Finite rate chemistry
• Conserved Scalar Equilibrium model	• Flamelet model • Linear Eddy model • Probability Density Function (PDF) model • Conditional Moment Closure (CMC) model • Multiple Mapping Conditioning (MMC) model

Table 2.2 [12] reviews list of important turbulent combustion models for non-premixed combustion for the two categories. It should be mentioned that some of these models like the PDF model and Linear Eddy model, are applicable for premixed combustion as well. In the following sections of this chapter, these non-premixed combustion models are briefly reviewed.

2.5. Flamelet model

The Flamelet model for non-premixed combustion describes the turbulent flame as a collection of laminar flame elements. Peters [27] and Kuznetsov [28] independently derived Flamelet equations based on the mixture fraction. In fact, mixture fraction decouples the turbulent transport and the flame structure.

The scalar dissipation rate is an important parameter in Flamelet model. It represents the inverse of diffusion time scale and relates to the flow velocity gradients.

Separation of the complex chemical structure from the flow dynamics of the flames is the main advantage of the Flamelet model. However, steady Flamelet model is limited to fast chemistry flames. So the non-equilibrium effects like ignition and extinction cannot be captured by this model.

2.6. Conditional Moment Closure (CMC) model

Conditional Moment Closure (CMC) was conceptually derived as a mixture fraction based approach for non-premixed turbulent combustion by Klimenko [29] and Bilger [30].

Exploiting a strong correlation between reactive scalar species and the mixture fraction is the basic idea behind CMC approach for non-premixed combustion. As a result, there is a correlation between fluctuations of reactive scalars with respect to the mixture fraction fluctuation. Conditioning of the reactive species on mixture fraction then leads to relatively small fluctuations around the conditional mean and a simple first order closure for the chemical source term can be found. It should be mentioned that CMC was extended to premixed turbulent combustion with conditioning on a reaction progress variable in subsequent work [13] .

For a given scalar Y, we can decompose it into a mean and a fluctuation:

$$Y_k = \overline{Y}_k + Y_k' \qquad (2.20)$$

Fluctuations Y_k' are usually very strong in time and space, which makes the closure of chemical source term very difficult.

The alternative decomposition is

$$Y_k = \langle Y_k \,|\, z \rangle + Y_k'' \qquad (2.21)$$

Where z is the scalar sample space and Y_k'' is the fluctuation around the conditional mean or the *conditional fluctuation*. A basic assumption of the CMC method which is experimentally proven is that $Y_k'' << Y_k'$ [13].

The CMC transport equations for turbulent reacting flows were derived by Klimenko and Bilger [13] using somewhat different methodologies which are “the joint PDF method” and “the decomposition method” respectively.

The basic CMC transport equation for single conditioning on mixture fraction is as follow. This equation governs the evolution of conditional expectation $Q = \langle Y \,|\, \xi = \eta \rangle$ (where ξ is the mixture fraction and η is its sample space)

$$\rho_\eta \frac{\partial Q}{\partial t} + \langle \rho u_i \,|\, \eta \rangle \frac{\partial Q}{\partial x_i} = \rho_\eta N_\eta \frac{\partial^2 Q}{\partial \eta^2} + \langle w_k \,|\, \eta \rangle - \frac{1}{P_\eta} \frac{\partial}{\partial x_i} \left[\rho_\eta \langle u_i'' Y_k'' \,|\, \eta \rangle P_\eta \right] \qquad (2.22)$$

where $N = D(\nabla \xi)^2$ is the scalar dissipation, $u_i'' = u_i - \langle u_i \,|\, \eta \rangle$ is the velocity fluctuation about the conditional mean and subscript η indicating conditioning on mixture fraction.

The first order closure for chemical reaction is a good approximation in zones that are not close to extinction. The conditional velocity and the conditionally averaged scalar dissipation are unclosed terms that need to be modelled in CMC transport equation. These terms can be neglected under high Reynolds number and equal molecular diffusivity assumptions.

2.7. Probability Density Function (PDF) method

Probability Density Function (PDF) method [31], [32] is a very effective solution for the closure problems provided by averaging or filtering chemical source terms in chemically reacting turbulent flows.

Joint PDF methods are applicable for premixed, non-premixed and partially premixed combustion as they do not depend on the selection of the conserved scalar. Since the relationship between particle methods and PDF methods was established by Pope [14], particle methods have become a powerful approach for solving PDF transport equations.

The method discussed here is the transport equation for the joint pdf of velocity and reactive scalars. If we denote the set of reactive scalars by the vector ψ, then $P(V,\psi;x,t)$ is the joint pdf at point x and time t. There are several ways to derive the transport equation for the $P(V,\psi;x,t)$ [14]. Formulation of the PDF transport equation is presented below.

$$\frac{\partial \rho P}{\partial t}+\nabla\cdot(\rho V P)+(\rho g-\nabla\bar{p})\cdot\nabla_V P+\sum_{i=1}^{N}\frac{\partial}{\partial \psi_i}[\omega_i P] \tag{2.23}$$
$$=\nabla_V\cdot\left[\langle -\nabla\cdot\tau+\nabla p' \,|\, V\psi\rangle\right]-\sum_{i=1}^{N}\frac{\partial}{\partial \psi_i}\left[\langle\nabla\cdot(\rho D\nabla\psi_i)\,|\,V\psi\rangle\right]$$

here N is the number of reactive species, i is any reactive scalar, ∇_V denotes the divergence operator with respect to the components of velocity and angular brackets denote conditional averages with respect to fixed values of V.

The first two terms on the left hand side of equation (2.23) are the local rate of change and convection of the PDF in physical space respectively. The third term represents transport in velocity space by gravity and mean pressure gradient. The last term contains the

chemical source term. For complex chemical kinetics, the closed form of the source terms gives the transported PDF formulation great advantage over other formulations. All four terms on the left hand side are computed in physical space and are in closed form. On the right hand side of equation (2.23), the first term describes the transport of the PDF in velocity space caused by the viscous stresses and the fluctuating pressure gradient. The second term represents transport in reactive scalar space by molecular fluxes. This molecular mixing term is unclosed and needs mixing models. Therefore, the quality of the mixing models controls the predictive capability of the PDF transport equation.

The PDF transport equation, which is a partial differential equation, can be solved with finite volume or finite difference methods. Since computational cost increases approximately exponentially with the number of dimensions, these methods are not effective due to high dimensionality of PDF transport equations. Therefore, most numerical implementations of PDF methods for turbulent reactive flows employ Monte Carlo Lagrangian particle simulation techniques. While these methods are still computationally expensive, cost increases linearly with dimensionality of the problem.

In the Lagrangian approach, particles are not restricted to grid nodes. Lagrangian particles are notional, have a position, move through the computational domain with instantaneous velocity and are characterised by values of the reactive scalars. Although these particles behaved similarly to real fluid particle in some way, they should not confused with them [12]. In some publications, Lagrangian particles are termed Pope particles [33] .

The concept of the particle approach is to develop a system of stochastic particles whose evolution yields the same one-point, one-time Eulerian PDF as a real fluid system. Models for notional particle interactions then effectively provide closure for the Eulerian PDF equations, and solving for the evolution of notional particles corresponds to solving a modelled PDF transport equation. The particle distributions are effectively determined by solving stochastic differential equations. The statistics of the turbulent reacting flow are represented by the estimation of the stochastic particle field.

Conventionally, in Lagrangian approach for turbulent combustion over one hundred particles are present in each cell. So for simulations of laboratory flames with grids with thousands of cells, this can result in the order of hundreds of thousands to tens of millions of particles [34]. Performing mixing and reactions over this huge number of particles is computationally expensive. Recent advances in PDF methods like those that improved mixing models in particle-based methods can consider as a remedy for this.

2.7.1. Filtered Density Function (FDF) method

The Filtered Density Function (FDF) method is an approach to extending PDF-based modelling to the LES method. The main advantages of FDF method, same as PDF method, are that the chemical source term remains in closed form. The FDF method was introduced by Pope [35], and a transport equation for a composition FDF first was derived and modelled by Gao [36].

The procedures of driving FDF transport equations are very similar to the approach used for driving PDF transport equations and the resulting equations of both models have the same structure.

However, there are two main differences between PDF and FDF methods. First, the mean quantities in the PDF equations are replaced by spatially filtered quantities in the FDF equations. Second, the sub-filter turbulence scales in FDF equations replace the mean-quantity-based turbulence scales in PDF equations.

A review of developments and applications of FDF method can be found in Drozda et al. [37].

2.7.2. Different mixing models

Mixing models are a central research topics of lots of transport PDF/FDF methods. The most essential characteristics of scalar mixing models for PDF methods proposed by Subramanian and Pope [38] are as follows:

- **Conservation of Means:** The mean quantities of scalars should not be affected as a result of mixing
- **Decay of Variances:** Scalar variances should decay at the correct rate due to mixing process.
- **Boundedness:** Scalar quantities should remain bounded due to conservation of mass. It is necessary for all scalars to remain between the minimum and maximum values.
- **Linearity and Independence:** The set of governing equations of scalar fields is linear with respect to the scalar fields. This linearity criteria should keep unchanged

during mixing process when the scalars are subject to linear transformation. Additionally, the evolution of each scalar field should be independent from others.

- **Relaxation to Gaussian:** In homogeneous isotropic turbulence, the mixing model should relax a scalar PDF towards a Gaussian distribution as is indicated by both experiments and DNS results.

- **Localness:** Mixing of scalars should be governed by their presence in a composition and scalar space.

The commonly used particle mixing models for Lagrangian particles are summarised below.

Interaction by Exchange with the Mean (IEM) [31] - The IEM model is the simplest mixing model which relaxes all scalar values to the local mean. IEM model possess the first three characteristics but is not local in the composition space.

Modified Curl's model [39] - The Modified Curl mixing model is a particle interaction model based on Curl's model [40] where mixing takes place between randomly selected particle pairs. This model, similar to the IEM model, is nonlocal in composition space.

Mapping closure [41] - In this model the scalar field is mapped to a Gaussian reference field. Mapping closure is local in reactive scalar space.

Euclidean Minimal Spanning Tree (EMST) [38] - The basic idea of the EMST model is that mixing of scalar particles should be governed by those in their close neighbourhood in reactive scalar space. This model does not satisfy the linearity and independence principles.

Shadow Position Mixing Model (SPMM) [42] - This model conceptually addresses issues related to combining conditioning of mixing with spatial transport properties. SPMM performs conditioning based on taking into account alternative trajectories of Lagrangian particles in a turbulent flow. Depending on exact implementation, this model may perform as original MMC or as generalised MMC that will be discussed more in section 2.8.

2.8. Multiple Mapping Conditioning (MMC)

2.8.1. Overview and basic concept of MMC model

Multiple Mapping Conditioning (MMC) was introduced by Klimenko and Pope in 2003 [16] as a new turbulent combustion modelling framework that unifies the features of the PDF model and CMC model by incorporating a generalised mapping closure method.

MMC developed in order to improve modelling efficiency by manifold reduction. The idea is that while the complete composition space in a turbulent flow is highly dimensional, it is not necessary in a practical model to allow all species to fluctuate in all possible directions. This concept leads to projection of a full dimensional composition space to a reduced dimensional manifold.

There are two methodologies in this regards to investigate. The first one is achieved by reducing the number of species in the chemical kinetics scheme. Intrinsic Low-Dimensional Manifold (ILDM) suggested by Mass [43] is a primary example of this method. The second approach is deriving transport equations that effectively restrict the compositions to a certain manifold. CMC and Flamelet models are examples of the latter methodology. With its reduced manifold consisting of reference variables, MMC belongs to the second methodology as well.

The main idea of MMC is modelling turbulent fluctuations and micro mixing in physical composition space by using turbulent fluctuations and micro mixing in a reference space with a known PDF.

The *major* and *minor* spices terms are introduced into the MMC model while the term species can include chemical species, mixture fraction, enthalpy as well as other related quantities. The reference space is determined by the *major* manifold and its turbulent fluctuation is considered as *major fluctuation* where can freely fluctuate in any physically way. The remaining minor species are only permitted to fluctuate jointly with the major species and are therefore conditioned on the mean concentrations of the major species [44].

Beginning with original MMC in this section, two MMC subsets, deterministic and stochastic MMC, and generalised MMC will be discussed briefly in next two sections.

2.8.2. Deterministic and stochastic MMC model

MMC was proposed with both deterministic and stochastic formulations by Klimenko and Pope [16].

Deterministic MMC was the natural extension of CMC with a consistent closure of the mixture fraction PDF and conditional mean scalar dissipation. Stochastic MMC was first derived as a stochastic realization of the deterministic MMC for numerical efficiency only. By adopting a probabilistic interpolation, stochastic MMC is in fact a complete joint PDF method with MMC enforcing CMC properties on the mixing model by using reference variables to emulate turbulence properties and localised mixing in the reference variable space.

In fact, in the probabilistic MMC model, the dissipation of minor fluctuations is modelled by mixing between particles in a close neighbourhood in reference variable space, which gives MMC its localness. In conventional joint PDF methods the mixing models account for the dissipation of all fluctuations, whereas in MMC the mixing operator dissipates only the minor fluctuations and the dissipation of major fluctuations is modelled by diffusion in reference space.

2.8.3. Generalised MMC and Sparse- Lagrangian Simulation

Generalised MMC was first proposed by Klimenko in 2005 [45] in order to develop the reference variables concept beyond conditioning or localisation in MMC method.

In this more flexible MMC version, severe restrictions on the formulation of reference variables are removed. In the original stochastic MMC, all reference variables are modelled by Markov processes. Although, using a standard Gaussian distribution to model reference variables is conventional and mathematically convenient, it is not necessarily a good model for the physical property of interest. In generalised MMC, reference variables can be modelled by any physically relevant process. Therefore, by obtaining reference variable from resolved LES fields at an instant, generalised MMC can build a very computationally efficient method for solving FDF equations.

As discussed before, Lagrangian particle methods are used to solve FDF transport equations. In conventional Lagrangian approaches, the target is to reproduce the joint composition PDF in every Eulerian cell. Hence, mixing is between particles within the same Eulerian cells and many particles per cell are required. Application of this intensive

method to large-scale practical cases is not feasible with current computing power. For example, for a laboratory scale flame, simulations require one or two million LES grid cells but as many as 15 to 50 million Lagrangian particles.

Sparse models, on the other hand, are characterised by a relatively small number of Lagrangian particles used in simulations which results in similar reduction of the computational cost.

It must be emphasised that there are two mixture fractions in sparse-Lagrangian simulations. The first one is the mixture fraction, $\tilde{f}$, given by solving the balance equation in the LES scheme which is used as reference mixture fraction and enforces localisation in the MMC mixing model. The second one is the stochastic mixture fraction, z, used for evaluating the reactive scalar field.

The instantaneous Eulerian FDF transport equation can be recast into the form of the following stochastic differential equations that govern the evolution of the PDF:

$$dx_i^* = \left[\tilde{u}_i + \frac{1}{\overline{\rho}} \frac{\partial}{\partial x_i} (\overline{\rho}(D + D_t)) \right] dt + \delta_{ij} \sqrt{2(D + D_t)} \omega_j^* \qquad (2.24)$$

$$dY_i^* = (W_j^p + S_i^*) dt \qquad (2.25)$$

where $\tilde{u}_i$ is the filtered velocity, W is the reaction rate, D is the molecular diffusivity, D_t is the Smagorinsky turbulent diffusivity , ω is a Gaussian Weiner process and S_i is the mixing operator which emulates subgrid scale scalar dissipation.

The MMC-Curl's mixing model is similarly to Curl's model, but the particle pairs are selected specifically rather than randomly .The sparse-Lagrangian MMC approach in LES for non-premixed flames introduces a metric that defines the effective distance between particles p and q in an extended space of physical location and reference mixture fraction by

$$\hat{d}_{(p,q)}^2 = \left[\sum_{j=1}^{3} \left(\frac{\sqrt{3} d_{x_j^*}^{p,q}}{r_m} \right) + \left(\frac{d_{f^*}^{p,q}}{f_m} \right) \right] \qquad (2.26)$$

where asterisks denote stochastic quantities, $d^{p,q}_{x^*_j}$ and $d^{p,q}_{f^*}$ are the absolute distances between particle pairs in physical space and reference mixture fraction space, respectively. r_m and f_m are global characteristic scales whose ratio f_m / r_m controls the degree of MMC localisation. f_m is treated as a free parameter while the choice of r_m is constrained by a fractal/gradient model as discussed by Cleary and Klimenko [46].

2.9. Summary

As discussed in this chapter, the modelling of turbulent combustion is based on the numerical solution of a set of partial differential conservation equations. Out of the different modelling approaches, MMC which is the subject of this thesis, combines the joint PDF and CMC methods while inheriting the advantages of both. The use of reference variables is the common feature to both original and generalised versions of MMC model. MMC essentially enforces the desired conditional properties on the mixing operation.

Therefore, considering its features, the development of the MMC model is pursued in this thesis in order to emulate differential diffusion effects. It should be mentioned that differential diffusion is neglected in the original version of MMC.

The overview and literature of differential diffusion is discussed in the next chapter while the theoretical features and implementation of MMC model for differential diffusion are addressed in Chapter 4.

Chapter 3 - Differential Diffusion

3.1. Overview

In theoretical models of turbulent combustion, a great simplification is introduced by assuming that the molecular diffusivity of all species is equal. For instance in the mixture fraction based methods of non-premixed flames, based on the above assumption, mixture fraction is the single conserved scalar that can completely describe the state of mixing.

On the other hand, there exist numerous investigations on the subject of *differential diffusion* effects in turbulent combustion; over four decades evidence indicates a strong impact of differential diffusion for some flows. Such flows include turbulent flows with low to moderate Reynolds number, non-reacting laboratory flows and flames containing species like hydrogen, which has a higher diffusivity than other species while molecular transport plays an important role.

For better understanding of the significant effects of differential diffusion on flow quantities, the energy and variance spectrums of turbulent flow should be considered. Both kinetic energy and variance spectrums behave based on Kolmogorov's eddy cascade hypothesis. The energy spectrum dissipates by viscosity at the Kolmogorov scale, while scalar variance dissipation depends on Schmidt number. It can occur at equal (Sc of O (1)), smaller or larger length scales than Kolmogorov dissipation length scale. More details in this area discussed in Chapter 2.

Thus, it can be expected that for hydrogen containing species, $Sc \ll 1$, molecular transport has great effects on the low wave number end of the spectrum.

In light of the above discussion, it is clear that neglecting differential diffusion effects is not valid for all flows. Thus, understanding the physics of differential diffusion in depth as well as improving predictive turbulent combustion models to account for differential diffusion effects motivate several studies on the subject.

Numerical, experimental and model-development works on differential diffusion have been reviewed in this chapter. As non-premixed combustion is the focus of the present research, most of following cited investigations fall in this category .While the effect of differential diffusion on premixed flames are also significant and discussed in many publications.

3.2. Literature review

Differential diffusion in early stages observed by Bilger [47] while studying the methane diffusion flame data of Tsuji and Yamaoka [48]. Subsequently, Bilger and Dibble [49] described differential diffusion theoretically and developed equations to quantify its effects in turbulent diffusion flames. The differential diffusion variable, $Z = \xi_i - \xi_j$, is defined in this study as difference in two species mixture fractions (ξ_i and ξ_j).This variable is used to quantify differential diffusion effects in many studies in literature.

3.2.1. Numerical study

Direct numerical simulations (DNS) of differential diffusion in homogenous isotropic turbulent are performed by Yeung and Pope [17]. The complete de-correlation of two scalars with identical initial conditions due to different in their molecular diffusivity is observed. It was also shown that during the initial stages of mixing, only the small scales of the scalars are affected by differential diffusion. Effects on large scales indicated in the late stages of mixing.

Yeung and coworkers [50] performed another DNS work of a spectral study of differential diffusion in stationary, isotropic turbulence. It was observed that in the presence of mean scalar gradient, as a source of scalar production, differential diffusion only affected small scales. While in decaying scalar fields, the whole spectrum, from the small to the large scales were affected.

Nilsen and Kosaly [51] performed a DNS study in a decaying isotropic turbulence field. The scalar de-correlation is captured in their study as well.

Kerstein et al. [52] predicted the mean square of the conserved scalars differences is proportional to $\mathrm{Re}^{-0.5}$ while validating the results with numerical simulation.

Jaberi et al. [53] investigated DNS of the binary mixing of two scalars with unequal molecular diffusion coefficients. The simulation was performed in both non-reacting and reacting homogeneous turbulent flows with and without the presence of mean scalar gradients. The complexity of the coupled influences of differential diffusion and chemical reaction was indicated.

A DNS study of Reynolds number scaling of passive scalars in statistically stationary homogeneous turbulence has also been conducted by Smith [54].

Nilsen and Kosály [55] presented DNS examining differential diffusion effects on reacting scalars in isotropic, decaying turbulence with one-step, isothermal reaction. Results demonstrated decreasing of effects with increasing Reynolds number.

Yeung and coworkers [56] , [57] expanded previous DNS studies for higher Reynolds and Schmidt numbers.

The above DNS simulations of differential diffusion provide sufficient data for comparison purposes.

3.2.2. Experimental works

There are numerous experimental studies of differential diffusion effects in both reacting and non-reacting flows in literature.

Drake et al. [58] , [59] investigated differential diffusion experimentally in a non-reacting jet flame of H_2 in air with Reynolds number of 1500 and up to 8500 respectively.

Masri et al. [60] showed the differential diffusion effects of hydrogen/carbon dioxide turbulent nonpremixed flame. The joint Raman-Rayleigh-LIF technique is used.

Smith et al. [61] studied non-reacting jets of H2/CO2 into air over a range of Reynolds numbers from 1000 to 64000. Pulsed laser Raman scattering spectroscopy is used to measure species concentrations. Measurements of average species concentrations showed significant differential diffusion effects in a laminar jet (Re=1000) while in jet flows of higher Reynolds numbers, only instantaneous species concentrations are affected by differential diffusion.

Measurement of differential diffusion of a non-reacting propane-helium jet flowing into air is presented by Su [62]. Planar Rayleigh scattering at Reynolds numbers ranging from 1000 to 3550 is used in this experiment. It is found that the root- mean- square of the differential diffusion variable , Z , varied as $\mathrm{Re}^{-0.47}$ in this flow which is similar to the prediction of Kerstein et al. [52].

A series of laser Rayleigh-scattering experiments at various Reynolds numbers in a turbulent non-reacting jet flow of Freon and Hydrogen into co-flowing air was performed for showing differential diffusion effects by Dibble and Long [63].

Study of differential diffusion in a turbulent jet of high-Schmidt-number scalars , between 2000 and 50000, was performed by Lavertu et al. [64]. In this work the root-mean-square of normalized concentration difference of scalars was shown to scale as $\mathrm{Re}^{-0.1}$, similar to the prediction of Fox [65].

Brunel and Su [66] described quantitative measurements of the differential diffusion variable in a turbulent propane-helium jet issuing into air. Planar laser Rayleigh scattering is used for jet exit Reynolds number ranges from 1000 to 3000.

Several researchers have experimentally studied differential diffusion effects in reacting flows.

Smith et al. [67] measured temperature and species concentrations in reacting jets of H_2/CO_2 into air over a range of jet Reynolds numbers from 1000 to 30000 using Pulsed Raman Scattering spectroscopy.

Bergmann et al. [68] and Meier et al. [69] also investigated differential diffusion effects of reacting jet diffusion flames in different Reynolds numbers.

3.2.3. Model Developments

Many publications consider differential diffusion in the context of different turbulent combustion models.

Bilger and Dibble [49] studied differential diffusion in a jet of hydrogen and propane at a Reynolds number of 2700 by using a $k-\varepsilon$ model.

Kerstein [70] and Kerstein et al. [52] used the linear-eddy model to study differential diffusion. In the former study, a turbulent jet of a hydrogen/propane mixture at Reynolds numbers of 5000 and 20000 is simulated. In the latter one, the Reynolds number ranged from 100 to 8000 for scalars with Schmidt number ranging from 0.01 to 1 is investigated. The results showed the differential diffusion variable variance scaled as $\mathrm{Re}^{-0.5}$.

Kronenburg and Bilger [71] developed a Conditional Moment Closure (CMC) model to account for differential diffusion effects for non-reacting and for reacting flows [72]. It is discussed that when considering differential diffusion, the terms involving the fluctuations around the conditional means in CMC transport equation, the e_y-terms, need modeling and cannot be neglected

A Flamelet [11] , [73] model for inclusion differential diffusion is improved by Pitsch and Peters [74] and Pitsch [75] by applying a Lagrangian Flamelet model to a steady, turbulent $CH_4/H_2/N_2$–air diffusion flame.

Sannan and Kerstein [76] , [77] employed the LEM3D model based on the Linear Eddy Model (LEM) to simulate differential diffusion effects in a turbulent round jet of Hydrogen and Freon 22 into air.

A number of differential diffusion models for transported PDF methods are available in the literature as follow.

Chen and Chang [78] developed a method for stochastic mixing models and applied it in the modified Curl's [39] and IEM [79] mixing models The numerical results have been assessed by comparisons with experimental work of Smith et al. [61] , [67] with a fuel mixture of 36% H_2 and 64% CO_2 and the Meier et al. [69] with a fuel mixture of 50% H_2 and 50% N_2.

Fox [65] extended the Lagrangian Spectral Relaxation Model (LSR) for differential diffusion in forced homogeneous isotropic turbulence. Four different values of turbulence Reynolds number, Re=538, 90, 160, and 230, with and without uniform mean scalar gradients were used. Results predicted the $\mathrm{Re}^{-0.3}$ scale for variance of the scalar difference which is weaker than decay predicted by Kerstein et al. [52]. This difference can be attributed to backscatter, which its rate from the diffusive scales towards the large scales was found to be the key parameter in this model.

McDermott and Pope [80] presented a new approach in PDF methods for treating differential spatial diffusion. The IEM model [79] was used for mixing in this study.

Richardson and Chen [81] proposed an approach for differential diffusion of turbulent premixed methane–air combustion which ensured reliability of mixing. The method is applied in the IEM [79] and the Euclidean Minimum Spanning Tree (EMST) [38] models.

Chapter 4 - A Multiple Mapping Conditioning model for differential diffusion

Chapter 4 is to achieve the main objective of this research, which is developed Multiple Mapping Conditioning (MMC) model in order to account for differential diffusion effects.

4.1. Paper 1 - A multiple mapping conditioning model for differential diffusion

A multiple mapping conditioning model for differential diffusion

L. Dialameh,[1] M. J. Cleary,[2] and A. Y. Klimenko[1])

[1]*School of Mechanical and Mining Engineering, The University of Queensland,*

Queensland 4072, Australia

[2]*School of Aerospace, Mechanical and Mechatronic Engineering, The University of Sydney,*

New South Wales 2006, Australia

(Received 15 August 2013; accepted 22 January 2014; published online 12 February 2014)

This work introduces modelling of differential diffusion within the multiple mapping conditioning (MMC) turbulent mixing and combustion framework. The effect of differential diffusion on scalar variance decay is analysed and, following a number of publications, is found to scale as $Re^{-1/2}$. The ability to model the differential decay rates is the most important aim of practical differential diffusion models, and here this is achieved in MMC by introducing what is called the *side-stepping method*. The approach is practical and, as it does not involve an increase in the number of MMC reference variables, economical. In addition, we also investigate the modelling of a more refined and difficult to reproduce differential diffusion effect – the loss of correlation between the different scalars. For this we develop an alternative MMC model with two reference variables but which also makes use of the side-stepping method. The new models are successfully validated against DNS results available in literature for homogenous, isotropic two scalars mixing.

I. Introduction

Fundamental studies of turbulent mixing are of importance to a broad range of engineering disciplines such as combustion, environmental fluid dynamics and chemical processing. Due to the complexity of turbulent flows, the majority of fundamental scalar mixing studies consider the evolution of a single scalar only. In practice, of course, more than one scalar is usually mixed. For example, the structure of a turbulent flame is strongly influenced by the complex reactive-diffusive interactions involving numerous chemical species. In general, each scalar has its own molecular diffusivity and may evolve differently to other species due *differential diffusion*. This effect is most noticeable in flows where turbulent mixing is less dominant than molecular mixing; for example in low Reynolds number flows and small scale mixing processes. Differential diffusion is especially important in mixtures containing species that are substantially more or less diffusive than the other constituents. An example of this latter case is the combustion of hydrogen. Due to the high diffusivity of hydrogen relative to other species (because its much lower molecular weight) and the importance of hydrogen containing species on carbon monoxide oxidation, it is speculated that differential diffusion plays an important role in the burn-out of carbon monoxide (a dangerous pollutant), and also in flame extinction and re-ignition processes which affect combustor stability [78]. The ability to predict these effects is increasingly important as the focus turns to hydrogen containing fuels such as syngas. However, many existing predictive models neglect differential diffusion. This has usually been based on the assumption that turbulent mixing is dominant over molecular mixing thus simplifying the theory behind many turbulent mixing models and becoming an integral part of them. In light of the above discussion it is apparent that this assumption is not valid for all flows thus motivating several studies to better understand the physics of differential diffusion and to suggest improved predictive models. A brief review follows.

A number of differential diffusion models for transported probability density function (PDF) [14]' [82] methods are available in the literature. Chen and Chang [78] develop a method for stochastic mixing models and demonstrate its application in the context of the modified Curl's [39] and IEM [79] mixing models. A differential diffusion form of the Lagrangian spectral relaxation (LSR) model is developed by Fox [65]. More recently McDermott and Pope [80] consider the inclusion of differential spatial diffusion, while Richardson and Chen [81] propose a new approach for treating differential diffusion using both the IEM and Euclidean minimum spanning tree (EMST) [38] micro-mixing models. Various publications consider differential diffusion in the context of other combustion models; Kronenburg and

Bilger [71] , [72] and Smith [54] extend conditional moment closure (CMC) [13] to account for differential diffusion while differential diffusion in flamelet [11] , [73] models are reported in Pitsch and Peters [74] and Pitsch [75]. Differential diffusion for the linear-eddy model and the eddy-damped quasinormal Markovian (EDQNM) model are developed by Kerstein [70] and Ulitsky et. al. [83], respectively. Theoretical and DNS investigations of differential diffusion are also widely reported. Following on from Bilger's [47] observation of differential diffusion effects in methane diffusion flames, Bilger and Dibble [49] introduce a differential diffusion variable that is the difference between two mixture fractions (or passive scalars). That quantity is subsequently used by Kerstein et al. [52] in their analysis of the Reynolds number scaling of differential diffusion, and in a series of DNS studies by Yeung and coworkers [17] , [50], [56], [18], Jaberi et al. [53] and Nilsen and Kosály [51] , [55]. Experimental studies of differential diffusion are reported for both reacting and non-reacting flows. For example, differential diffusion in non-reacting flows is explored by Drake et al. [59] , [58], Masri et. al [60], Smith et. al.[61] and Dibble and Long [63]. While reacting flows are considered by Smith et al. [67] and Bergmann et al. [68]. Most of the above cited works are for non-premixed combustion, which is also the focus of the present research, but it is noted that the effect of differential diffusion on premixed flames are significant and discussed in many publications (e.g. Kuznetsov and Sabelnikov [73]) but not specifically considered here.

In the present work, we develop an extension to the multiple mapping conditioning (MMC) model so that it too can account for differential diffusion effects. MMC, which was first derived by Klimenko and Pope [16], is a modelling framework for turbulent combustion which effectively unifies the features of CMC and PDF models. Deterministic and stochastic formulations of MMC have been derived and tested for various flame configurations; see Cleary and Klimenko [44] for a recent review. The stochastic formulation of MMC is a full-scale PDF method but one where turbulent mixing is local to a low-dimensional reference variable manifold. Mixing localness is a key principle of high quality turbulent mixing models [38] along with other important attributes also satisfied by MMC such as independence, linearity and relaxation to a Gaussian scalar distribution in homogeneous turbulence. For non-premixed combustion of equally diffusing species, it is possible to select a one-dimensional reference variable space representing mixture fraction. This effectively imposes a CMC-type closure onto a PDF model, giving MMC the advantages of both of those methods. MMC models with multiple-dimensional reference

variable spaces containing specific enthalpy and scalar dissipation [84] have also been developed for partially premixed combustion.

In general there are two aspects of molecular diffusion in PDF methods which need to be considered: the first is spatial transport [78] , [80], which appears in the PDF transport equation as gradient diffusion in physical space; and the second is the process of mixing of scalars at a fixed location [65] , [71] which appears as transport in composition space. Differential diffusion may affect both of these. Spatial transport by molecular diffusion can be significant in low Reynolds number turbulent mixing. Moreover, in large eddy simulations (LES) the locally dominant physical processes depend on the filter width and the local viscous length scale. When the filter width becomes small relative to the viscous scale, molecular diffusion needs to be considered. While an MMC-consistent treatment of differential spatial transport can be achieved with the use of the shadow position mixing model (SPMM), which has been recently suggested by Pope [85], the focus of this present study is on the effects of differential diffusion on the local mixing in composition space. We examine one-point joint characteristics and avoid complications associated with inhomogeneity and chemical reactions by considering differential diffusion of unreactive passive scalars in statistically-stationary, isotropic turbulent flow. Two different MMC models for treating differential diffusion are introduced: the first model has one reference variable and is able to predict the differential rate of decay of scalar variances, while the second model which has two reference variables is also able to predict the loss of correlation between differentially diffusing scalar fields.

The remainder of this paper is organised as follows. Fundamentals of differential diffusion are presented in Section II, covering the governing scalar transport equations and some new theory on the Reynolds and Schmidt number scaling of differential diffusion. In Section III extensions of the MMC model for differential diffusion are developed and validated against DNS results of Yeung and Pope [17] and Yeung and Luo [18]. The dependence of the model parameters on the Reynolds and Schmidt number are also demonstrated. Conclusions are drawn in section IV.

II. Fundamentals of differential diffusion

In this section, we present some fundamentals of turbulent mixing of differentially diffusing scalars. Part A presents the transport equations governing the advection-diffusion of two passive scalars in homogenous turbulent flow, along with equations for the transport of

their variances and covariance. In Part B the spectral view of diffusion, in general, and differential diffusion, in particular, is reviewed and in that context we analyse the Reynolds and Schmidt number scaling of differential diffusion.

A. Governing equations

We consider two passive scalars Y_I and Y_{II} in a homogeneous, isotropic turbulent flow with decaying turbulence and without a mean scalar gradient. This latter simplification allows the mean value of each scalar to be taken as zero without a loss of generality. Each scalar has a different molecular diffusivity denoted by D_I and D_{II}, respectively, with corresponding Schmidt numbers Sc_I and Sc_{II}. The fluctuations of each scalar evolve by the advection-diffusion equations

$$\frac{\partial Y_I}{\partial t} + u_i \frac{\partial Y_I}{\partial x_i} = D_I \frac{\partial^2 Y_I}{\partial x_i \partial x_i} \tag{4.1}$$

$$\frac{\partial Y_{II}}{\partial t} + u_i \frac{\partial Y_{II}}{\partial x_i} = D_{II} \frac{\partial^2 Y_{II}}{\partial x_i \partial x_i} \tag{4.2}$$

where $u_i = u_i(x)$ is the turbulent velocity field. The mean scalar variances $\langle Y_\mathrm{I}^2 \rangle$ and $\langle Y_\mathrm{II}^2 \rangle$ decay with time according to

$$\frac{\partial \langle Y_\mathrm{I}^2 \rangle}{\partial t} = -2D_\mathrm{I} \left\langle \left(\frac{\partial Y_\mathrm{I}}{\partial x_i} \right)^2 \right\rangle = -\chi_\mathrm{I} \tag{4.3}$$

$$\frac{\partial \langle Y_\mathrm{II}^2 \rangle}{\partial t} = -2D_\mathrm{II} \left\langle \left(\frac{\partial Y_\mathrm{II}}{\partial x_i} \right)^2 \right\rangle = -\chi_\mathrm{II} \tag{4.4}$$

where χ_I and χ_{II} are the scalar dissipation rates. The most important joint statistic is the covariance, $\langle Y_\mathrm{I} Y_\mathrm{II} \rangle$, which evolves according to

$$\frac{\partial \langle Y_\mathrm{I} Y_\mathrm{II} \rangle}{\partial t} = -2(D_\mathrm{I} + D_\mathrm{II}) \left\langle \frac{\partial Y_\mathrm{I}}{\partial x_i} \frac{\partial Y_\mathrm{II}}{\partial x_i} \right\rangle = -\chi_\mathrm{I,II} \tag{4.5}$$

Where $\chi_{\mathrm{I,II}}$ denotes the joint scalar dissipation. We also make use of the cross-correlation coefficient, $\rho_{\mathrm{I,II}}$, which is defined as

$$\rho_{\mathrm{I,II}} = \frac{\langle Y_{\mathrm{I}} Y_{\mathrm{II}} \rangle}{\left[\langle Y_{\mathrm{I}}^2 \rangle \langle Y_{\mathrm{II}}^2 \rangle \right]^{1/2}}. \tag{4.6}$$

B. Reynolds and Schmidt number scaling of differential diffusion

In this section, we first review the general spectral properties of turbulent scalar mixing before looking specifically at the spectra of two differentially diffusing scalars. Whereas much previous literature [49]' [51]' [65] '[52, 83] has chosen to quantify differential diffusion in terms of the difference of two passive scalars, we instead quantify differential diffusion in terms of the ratio of scalar dissipation timescales. The advantage is that this quantity is stationary in time. We develop relations for the Reynolds and Schmidt number scaling of the differential timescale ratio and make comparison to the scaling that is suggested in the previous literature.

The characteristic feature of any turbulent flow is the occurrence of eddies of different length scales. In decreasing order of size the four scales bounding different turbulent energy regimes are: the macroscale (L); the integral scale (l); the Taylor microscale (λ); and the Kolmogorov microscale (η). According to Kolmogorov's eddy cascade theory [86] the kinetic energy contained in the integral scale eddies is transferred down to the Kolmogorov scales where it is dissipated by viscosity. Turbulent fluctuations of transported scalars follow a similar cascade; the scalar variance generated at the large scales is transferred and dissipated by molecular diffusion at either the Batchelor or Oboukov-Corrsin scales depending on whether the molecular diffusivity is relatively larger or smaller than the kinematic viscosity (i.e. Schmidt number dependence). These dissipative length scales (η, η_B and η_{OC}) and their corresponding wavenumbers (k_K, k_B and k_{OC}) are as follows:

The Kolmogorov scale: $$k_K = \left(\frac{\varepsilon}{\nu^3} \right)^{1/4} = \frac{1}{\eta} \tag{4.7}$$

The Batchelor scale : $$k_B = \left(\frac{\varepsilon}{\nu D^2}\right)^{1/4} = k_K Sc^{1/2} = \frac{1}{\eta_B} \qquad (4.8)$$

The Oboukov-Corrsin scale: $$k_{OC} = \left(\frac{\varepsilon}{D^3}\right)^{1/4} = k_K Sc^{3/4} = \frac{1}{\eta_{OC}} \qquad (4.9)$$

where ε is the kinetic-energy dissipation rate, ν is the kinematic viscosity, D is the molecular diffusivity and $Sc = \frac{\nu}{D}$ is the Schmidt number.

Based on Kolmogorov's eddy cascade hypothesis [86], in the inertial subrange ($k_0 < k < k_K$) the turbulence is unaffected by viscosity and the kinetic energy spectrum scales according to the well-known $k^{-5/3}$ law. The scaling of the turbulent scalar spectrum is Schmidt number dependent. For $Sc < 1$, the scales are ordered as $k_{OC} < k_B < k_K$ and the scalars dissipate at Oboukov-Corrsin scale while the kinetic energy dissipates at the smaller Kolmogorov scale. Following Oboukov [21] and Corrsin [87] the passive scalar variance spectrum in the *inertial-convective* subrange ($k_0 < k < k_{OC}$) also follows a $k^{-5/3}$ rule

$$E_\theta(k) = C_1 \chi \varepsilon^{-1/3} k^{-5/3} \qquad (4.10)$$

where C_1 is the Oboukov-Corrsin constant. Alternatively, for $Sc > 1$ the wavenumber cut-offs are ordered as $k_K < k_B < k_{OC}$ and the scalar variance dissipates at the Batchelor scale while the turbulent kinetic energy dissipates at the relatively larger Kolmogorov scale. Batchelor [23] predicted that in the *viscous-convective* subrange ($k_{OC} < k < k_B$) the spectrum scales as

$$E_\theta(k) = C_2 \chi \left(\frac{\nu}{\varepsilon}\right)^{1/2} k^{-1} \qquad (4.11)$$

where C_2 is the Batchelor constant. It is noted that there are differences between gaseous and liquid flows. The former typically have Schmidt numbers of O(1) hence the dissipative Oboukov-Corrsin scale is of the same order as the Kolmogorov scale, and the later typically have Schmidt numbers of O(10^3) hence the scalar dissipation extends to the dissipative Batchelor scale which is much smaller than the Kolmogorov microscale.

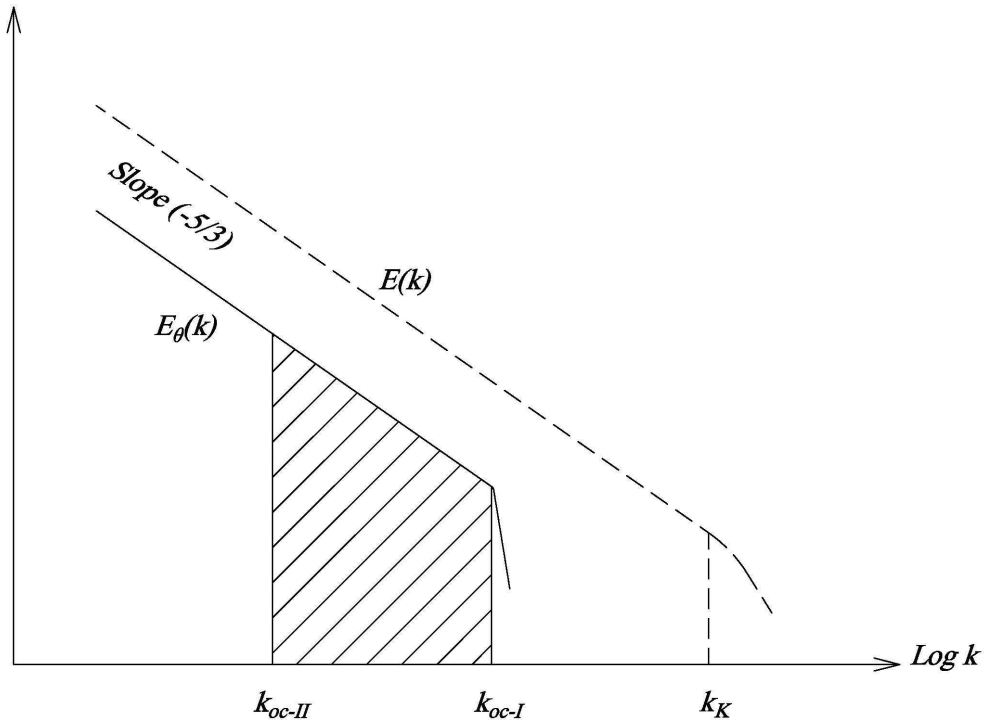

Figure 4.1. Energy and variance spectrum of two scalars with different diffusivity for the case $Sc_{II} < Sc_I \leq 1$

We now consider the spectral properties of two differentially diffusing scalars. For the passive scalars Y_I and Y_{II} introduced in the previous section, the scalar dissipation time scales are defined as

$$\tau_I = \frac{2\langle Y_I^2 \rangle}{\chi_I} \tag{4.12}$$

$$\tau_{II} = \frac{2\langle Y_{II}^2 \rangle}{\chi_{II}} \tag{4.13}$$

In general, two scalars with different dissipation times may have scalar dissipations and scalar variances, which are both different. For theoretical analysis, however, it is convenient to consider two scalars with different variances but the same scalar dissipation, $\chi_I = \chi_{II} = \chi$. Figure.4.1 illustrates the variance spectrum of the two scalars in the inertial-convective subrange for a low Schmidt number flow with $Sc_{II} < Sc_I \leq 1$. As discussed above, the dissipation occurs at the Oboukov-Corrsin scales denoted in wavenumber space by k_{OC-I} and k_{OC-II}. The scalar variance is equal to the integral over the entire wave number

space and therefore the difference between the two scalar variances (the cross-hatched area in Figure 4.1) is given by

$$\left\langle Y_I^2 \right\rangle - \left\langle Y_{II}^2 \right\rangle = \int_{k_{OC-II}}^{k_{OC-I}} E_\theta(k) dk \qquad (4.14)$$

Now, by substituting $E_\theta(k)$ from equation (4.10) into equation (4.14) we get

$$\left\langle Y_I^2 \right\rangle - \left\langle Y_{II}^2 \right\rangle = \frac{3}{2} C_1 \chi \varepsilon^{-1/2} \nu^{1/2} \left(Sc_{II}^{-1/2} - Sc_I^{-1/2} \right) \qquad (4.15)$$

Further, by substituting $\varepsilon = u^3 / l$, $\nu = ul/\mathrm{Re}_l$ and $T_l = l/u$ into equation (4.15), where u is the turbulent velocity, l is the integral length scale, Re_l is the integral Reynolds number and T_l is the integral time scale, and dividing the result by χ we get

$$\frac{\left\langle Y_I^2 \right\rangle}{\chi} - \frac{\left\langle Y_{II}^2 \right\rangle}{\chi} = \frac{3}{2} C_1 T_l \, \mathrm{Re}_l^{-1/2} \left(Sc_{II}^{-1/2} - Sc_I^{-1/2} \right) \qquad (4.16)$$

Next, substituting equations (4.12) and (4.13) on the left side of equation (4.16) then dividing both sides by T_l yields

$$\frac{\tau_I - \tau_{II}}{T_l} = 3 C_1 \, \mathrm{Re}^{-1/2} \left(Sc_{II}^{-1/2} - Sc_I^{-1/2} \right) \qquad (4.17)$$

loss of generality, we set $Sc_I = 1$ as a reference value. We also know that at high Reynolds number the ratio of the integral to dissipation timescales, T_l / τ_1, is a constant value [15, 88] which we will denote by C_3. With these last two simplifications we finally arrive at a low Schmidt number relationship for the ratio of the dissipation timescales as a function of Reynolds and Schmidt numbers

$$\frac{\tau_{II}}{\tau_I} = 1 - C \, \mathrm{Re}^{-1/2} \left(Sc_{II}^m - 1 \right) \qquad (4.18)$$

where $m = -1/2$ and $C = 3 C_1 C_3$

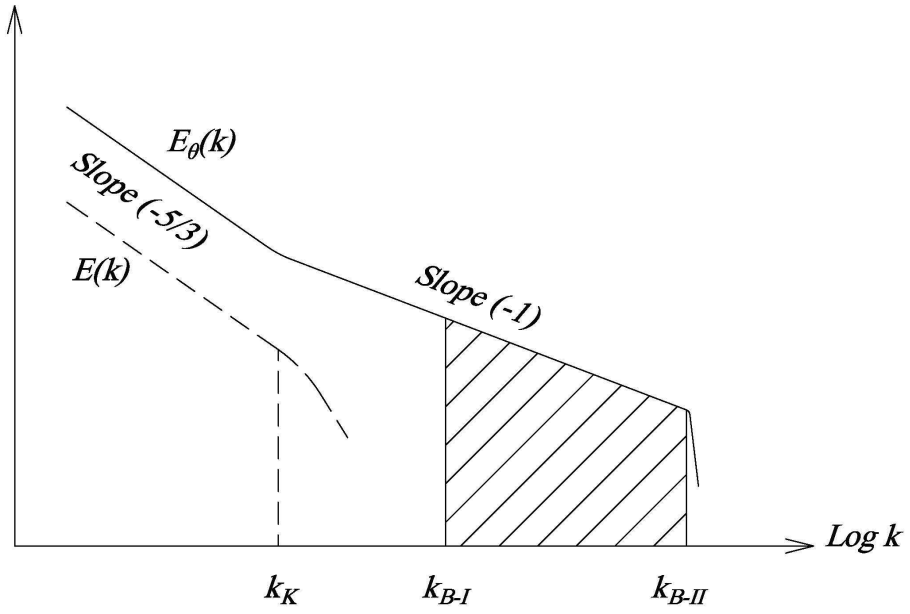

Figure 4.2. Energy and variance spectrum of two scalars with different diffusivity for the case $Sc_{II} > Sc_I > 1$

We now turn our attention to the high Schmidt number case with $Sc_{II} > Sc_I > 1$. Figure 4.2 illustrates the variance spectrum $E_\theta(k)$ for this case, showing both the $-5/3$ and -1 spectra and dissipation at the Batchelor scales, k_{B-I} and k_{B-II}. As before, the difference between the two scalar variances (the cross-hatched area in Figure 4.2) is given by

$$\left\langle Y_{II}^2 \right\rangle - \left\langle Y_I^2 \right\rangle = \int_{k_{B-I}}^{k_{B-II}} E_\theta(k) dk \qquad (4.19)$$

Substituting $E_\theta(k)$ from equation (4.11) into equation (4.19) gives

$$\left\langle Y_I^2 \right\rangle - \left\langle Y_{II}^2 \right\rangle = \frac{1}{2} C_2 \chi \varepsilon^{-1/2} \nu^{1/2} \left(\ln\left(Sc_{II}\right) - \ln\left(Sc_I\right) \right) \qquad (4.20)$$

and putting $\varepsilon = u^3/l$, $\nu = ul/\mathrm{Re}_l$ and $T_l = l/u$ into equation (4.20) and dividing by χ leads to

$$\frac{\left\langle Y_I^2 \right\rangle}{\chi} - \frac{\left\langle Y_{II}^2 \right\rangle}{\chi} = \frac{1}{2} C_2 T_l \,\mathrm{Re}_l^{-1/2} \left(\ln\left(Sc_{II}\right) - \ln\left(Sc_I\right) \right) \qquad (4.21)$$

Now, substituting equations (4.12) and (4.13) on the left side of equation (4.21) then dividing through by T_I while setting $Sc_I = 1$ (as previously explained) leads to the high Schmidt number relationship for the ratio of the dissipation time as a function of Reynolds and Schmidt numbers

$$\frac{\tau_{II}}{\tau_I} = 1 - C_2 \,\mathrm{Re}^{-1/2} \ln\left(Sc_{II}\right) \qquad (4.22)$$

It is interesting to compare the scaling developed above with other forms reported in the literature. We consider only the $Sc < 1$ case which is most typical of combustion gases. First we need to formulate our result in terms of the scalar difference, so following Bilger and Dibble [49] we define

$$z = Y_I - Y_{II} \qquad (4.23)$$

which is rearranged to

$$Y_I = Y_{II} + z \qquad (4.24)$$

Since the mean values of Y_I and Y_{II} are zero, the mean value of z is also zero and we simply find the variance of equation (4.24) as

$$\left\langle Y_I^2 \right\rangle = \left\langle Y_{II}^2 \right\rangle + \left\langle z^2 \right\rangle + 2\left\langle Y_{II} z \right\rangle \qquad (4.25)$$

Differential diffusion occurs in the wavenumber band that is larger than the dissipative Oboukov-Corrsin scale of the most diffusive scalar. So for the case being considered, fluctuations of z occur mainly for $k > k_{OC-II}$ (see Figure 4.1). Furthermore, if the hypothesis of stochastic independence of large-scale and small-scale fluctuations in turbulent flows is taken into account [73], we can assume that $\left\langle Y_{II} z \right\rangle \approx 0$ since the fluctuations of z overlap with fluctuations of Y_I but not with the fluctuations of Y_{II} (note that $\left\langle Y_I z \right\rangle \neq 0$). Upon substitution of this approximation and $\left\langle Y_{II}^2 \right\rangle / \left\langle Y_I^2 \right\rangle = \tau_{II}/\tau_I$ into equation (4.25) we find that

$$\frac{\tau_{II}}{\tau_I} - 1 \approx \frac{\langle z^2 \rangle}{\langle Y_I^2 \rangle} \tag{4.26}$$

Finally, by substituting equation (4.18) into equation (4.26) we get

$$\frac{\langle z^2 \rangle}{\langle Y_I^2 \rangle} \approx C \,\mathrm{Re}^{-1/2} \left(Sc_{II}^{m} - 1 \right) \tag{4.27}$$

This $\mathrm{Re}^{-1/2}$ scaling is consistent with the theory developed by Kerstein et al. [52] and later corroborated by the DNS of Nilsen and Kosály [51]. Reynolds number dependence is also analysed by Fox [65] for the study of differential diffusion in forced homogeneous isotropic turbulence and scales as $\langle z^2 \rangle \sim \mathrm{Re}^{-0.3}$ which is close to the $-1/2$ theoretical value discussed above. The literature contains far fewer studies of the Schmidt number scaling but the result in equation (4.27) with $m = -1/2$ seems to be consistent with the finding of Ulitsky et al. [83].

III. A MMC mixing model for differential diffusion

Extensions of MMC to account for the effects of differential diffusion are developed and tested against DNS data [17] , [18] for binary mixing of two scalars, Y_I and Y_{II} , with differential diffusivities characterized by Schmidt numbers $Sc_{II} < Sc_I \leq 1$. In Part A we present the basic MMC model. In Part B an extended MMC model with a single reference variable is developed for the prediction of differential decay of scalar variance. In Part C an alternative MMC model with two reference variables is developed. In addition to correct prediction of differential decay of variance this second model can also predict the rate of decorrelation of the differentially diffusing scalars. We also demonstrate correct Schmidt and Reynolds number scaling of the two models. Predictions for both differential decay of scalar variance and the rate of decorrelation are validated against two DNS with different Schmidt numbers [17]. Additionally decorrelation predictions are compared against three DNS over a range of Reynolds numbers [18].

A. The basic MMC model

In MMC (as in other PDF methods) the turbulent scalar fields, whose mean and covariance evolves according to equation (4.3) through equation (4.5), are modelled using

an ensemble of Pope particles which are notional particles which possess scalar quantities subject to a mixing operation [33]. In homogenous turbulence the passive scalars Y_I and Y_{II} are modelled by a discrete mixing operation. We use the MMC-Curl particle interaction mixing model whereby particles are mixed in pairs and evolve as

$$Y_I^{*,\text{new}} = Y_I^* (1-\alpha) + \hat{Y}_\text{I}\, \alpha \qquad \text{(4.28a)}$$

$$Y_{II}^{*,\text{new}} = Y_\text{II}^* (1-\alpha) + \hat{Y}_\text{II}\, \alpha \qquad \text{(4.28b)}$$

Here the asterisk denotes values assigned to individual Pope particles, the acute symbol indicates the two-particle average of the scalars prior to mixing and $\alpha \in [0,1]$ is the mixing extent which is related to the turbulent mixing timescale. The mixing operation should ideally satisfy the set of principles suggested by Subramaniam and Pope [38]. The most important of these, at least within the current context, are decay of variance consistent with equations (4.3) and (4.4) to a Gaussian distribution, linearity and independence of mixing, and localness in composition space. Traditional mixing models satisfy some but not all of these principles. Curl's model [40] satisfies linearity and independence but violates the localness requirement leading to significant over prediction of conditional fluctuations of reactive scalars in jet flames [46]. EMST is local and predicts Gaussian decay but violates linearity and independence. MMC, on the other hand, satisfies all of these principles. Localness is achieved in MMC by forcing mixing to be between pairs of particles which are local in a reference variable space. The reference variables are modelled to emulate the major statistics of the turbulent scalar fields but, at the same time, they are mathematically independent of the stochastic scalar values Y^*. Various types of MMC reference variables have been tested. In this work the reference variables, ξ, are modelled by Ornstein-Uhlenbeck processes [15] of the following form

$$d\xi = -\frac{\xi(t)}{\theta} dt + \left(\frac{2}{\theta}\right)^{1/2} dW(t) \qquad \text{(4.29)}$$

where W(t) is a Wiener process and θ the reference variable dissipation timescale.

In most conventional joint PDF models, the dissipation of scalar variance is controlled exclusively by the mixing model in equation (4.28) and the parameter α has a major influence. In this respect, MMC is substantially different. Mixing is local within a reference

space which has the effect of causing scalar fluctuations to decay towards the scalar mean that is conditionally averaged on that reference space. Therefore the parameter α is linked to what we call the *minor dissipation timescale,* denoted here as τ_D. Following Klimenko's analysis [45] of conditional dissipation in various mixing models, a new parameter γ is defined as

$$\gamma = 1 - (1 - \alpha)^2 \tag{4.30}$$

Its ensemble mean is a function of the numerical time step and minor dissipation timescale

$$\langle \gamma \rangle = \frac{4dt}{\tau_D} \tag{4.31}$$

The major dissipation of scalar variance occurs due to the diffusion in reference variable space and the parameter θ in equation (4.29) is called the *major dissipation timescale*. The MMC localness parameter, Λ, is defined as the ratio of the minor to major dissipation timescales, $\Lambda = \tau_D / \theta$. Of course, this interpretation of major and minor scalar fluctuations is made on the assumption that the reference space adequately represents the multidimensional space that is accessed by the fluctuating scalar field. The concepts of major and minor dissipation timescales are discussed in detail in previous publications [45].

B. A MMC model for predicting differential decay of scalar variance (one reference variable method)

The primary objective of any differential diffusion model, especially those for practical applications, is the ability to model the differential rates of decay of scalar variance. For this purpose we propose an MMC model where the mixing of both Y_I^* and Y_{II}^* is localised in the space of a single reference variable ξ_I which is modelled according to equation (4.29). The major dissipation time scale θ_I is related to the physical dissipation timescale, τ_I; the dissipation timescale for the less diffusive species Y_I^*. Conventionally these two values are close to each other and if θ_I is properly selected (below this is achieved by matching the modelled decay of Y_I^* to DNS data [17]) then the correct evolution of Y_I^* ensues. Since $Sc_{II} < Sc_I$ then $\tau_{II}/\tau_I < 1$ according to equation (4.18). The faster rate of

dissipation for Y_{II}^* is modelled by extending the mixing window for that scalar. Such an extension of the mixing window can be achieved in a number of practical ways; but here it is handled by taking an additional side step in time at which point the particle mixing pairs are reselected based on the updated reference variable field. The full implementation of the model is as follows. The reference variable ξ_I is advanced by a time increment dt at which point scalar Y_I^* is mixed after localizing in ξ_I-space. At that point ξ_I is advanced by a further time increment $dt_s = r_s dt$ at which point scalar Y_{II}^* is localised in the updated ξ_I-space and mixed. That second time increment is a temporary side step and r_s is so called side step parameter in this model. Essentially the side step increases the mixing of the more diffusive scalar by increasing the mixing window or the modelled time available in which mixing takes place. As described below r_s is modelled so that Y_{II}^* evolves correctly. After Y_{II}^* is mixed the side step of ξ_I is discarded and the simulation continues. The process is shown schematically in Figure 4.3.

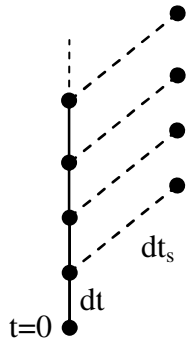

Figure 4.3. Conceptual sketch of the side-stepping method

It is emphasised that only the reference variable is modelled discontinuously and the conservation equations of the physical scalars Y_I and Y_{II} are not violated.

In this model the major dissipation time θ_I determines the variance decay rate of the less diffusive species while r_s determines the differential decay rate and in turn the decay rate of the more diffusive species. For closure, therefore, we require a model for r_s. First, we note the existence of the additional diffusion in reference space, which is associated with mixing. The intensity of this diffusion is given by [89]

$$D_m = \frac{d_m^2}{\tilde{\beta}\tau_D}, \quad \tilde{\beta} = \frac{\langle 1-\alpha^2 \rangle}{\langle 1-\alpha \rangle} \tag{4.32}$$

where D_m is the corresponding effective diffusion coefficient and d_m^2 is the square of the characteristic distance between mixing particles. In the side stepping model, there is an increase in the mixing window by an additional side step of dt_s which results in additional stirring of the particles leading to

$$d_m^2 = d_0^2 + 2Bdt_s \tag{4.33}$$

where d_0^2 is the average of the square distance between nearest particles. In the present work where a large number of particles are used in order to minimize stochastic errors, we can assume that d_0^2 is negligible in comparison with the term $2Bdt_s$ in equation (4.33). In cases with larger inter-particle spacing, for example sparse-Lagrangian MMC simulations, d_0^2 is finite and the numerical diffusion associated with that should be taken into account [33]. Hence, additional diffusion is created without varying the mixing extent α. As a result, the effective diffusion coefficient after side stepping and mixing is equal to

$$B_s = B + D_m \tag{4.34}$$

where $B = 1/\theta_I$. Substituting equation (4.32) into equation (4.34) where $dt_s = r_s dt$ and τ_D is substituted from equation (4.31) we have

$$\frac{B_s}{B} = \frac{\tau_I}{\tau_{II}} = 1 + r_s \frac{\langle \gamma \rangle}{2\tilde{\beta}} \tag{4.35}$$

This last equation is the relationship between scalar dissipation time scale ratio and the side step parameter r_s. From equation (4.18) we see that this ratio is also related to the physical flow properties, characterized by the Reynolds and Schmidt numbers. By substituting equation (4.35) into equation (4.18) the side stepping parameter is itself related to the flow physics by

$$r_s = \left(\frac{2\tilde{\beta}}{\langle\gamma\rangle}\right)\left(\frac{C\,\mathrm{Re}^{-1/2}\left(Sc_{II}^{m}-1\right)}{1-\left(C\,\mathrm{Re}^{-1/2}\left(Sc_{II}^{m}-1\right)\right)}\right) \qquad (4.36)$$

The MMC model developed above is now validated against the DNS data of Yeung and Pope [17] for the binary mixing of two differentially diffusing scalars in statistically stationary, homogeneous, isotropic turbulence. Two different DNS simulations are considered; in the first the scalar pairs have $Sc_I = 1$ and $Sc_{II} = 0.25$ while in the second simulation $Sc_I = 1$ and $Sc_{II} = 0.5$. The flow has a Taylor Reynolds number of $\mathrm{Re}_\lambda = 38$, an integral Reynolds number of $\mathrm{Re}_l = 216.6$ and an eddy turn-over time of 62.5s. The MMC simulations are performed using 10,000 Pope particles and a numerical time step of 0.1s. Additional simulations with as many as 30,000 Pope particles and with a numerical time step of 0.01s indicated that the results are relatively insensitive to changes in the numerical setup. Although a large number of particles are used in these simulations, so that time resolved variances and covariances can be obtained with small stochastic errors, practical implementations of the model within a CFD solver would typically use far few particles. The scalar fields are initialized by $Y_I^* = Y_{II}^*$ and given a standard normal distribution such that $\left\langle Y_I^* \right\rangle = \left\langle Y_{II}^* \right\rangle = 0$ and $\left\langle Y_I^{*2} \right\rangle = \left\langle Y_{II}^{*2} \right\rangle = 1$. Similarly, the reference variable is initialized with a standard normal distribution. The MMC localness parameter, Λ, the constant, *C*, in equation (4.36) and the mixing extent α are the three model parameters requiring explicit selection. The first is a time-invariant quantity whose value can be flow dependent [45]. Here it is selected manually so that the decay of $\left\langle Y_I^{*2} \right\rangle$ matches the DNS data while the decay of $\left\langle Y_{II}^{*2} \right\rangle$ is modelled implicitly through the side stepping process with r_s given by equation (4.36). The value of α is not critical and any value (or even random values [90]) between 0 and 1 can be used since the other parameters $\langle\gamma\rangle$ and $\tilde{\beta}$ in equation (4.36) will be correspondingly adjusted through equations (4.30) and (4.32). The results presented in this work are for $\alpha = 0.02$.

Figure.4.4 shows the scalar variances versus normalized time which is defined as the simulation time divided the DNS eddy turn-over time. The results for the two simulations with ($Sc_I = 1$, $Sc_{II} = 0.25$) and ($Sc_I = 1$, $Sc_{II} = 0.5$) are shown on the same set of axes. As can be seen the dissipation of scalar fluctuations by mixing occurs at different rates due to

their different diffusivities. The results show exponential decay of the variances, indicated by approximately straight lines of constant slope on the linear-log plot

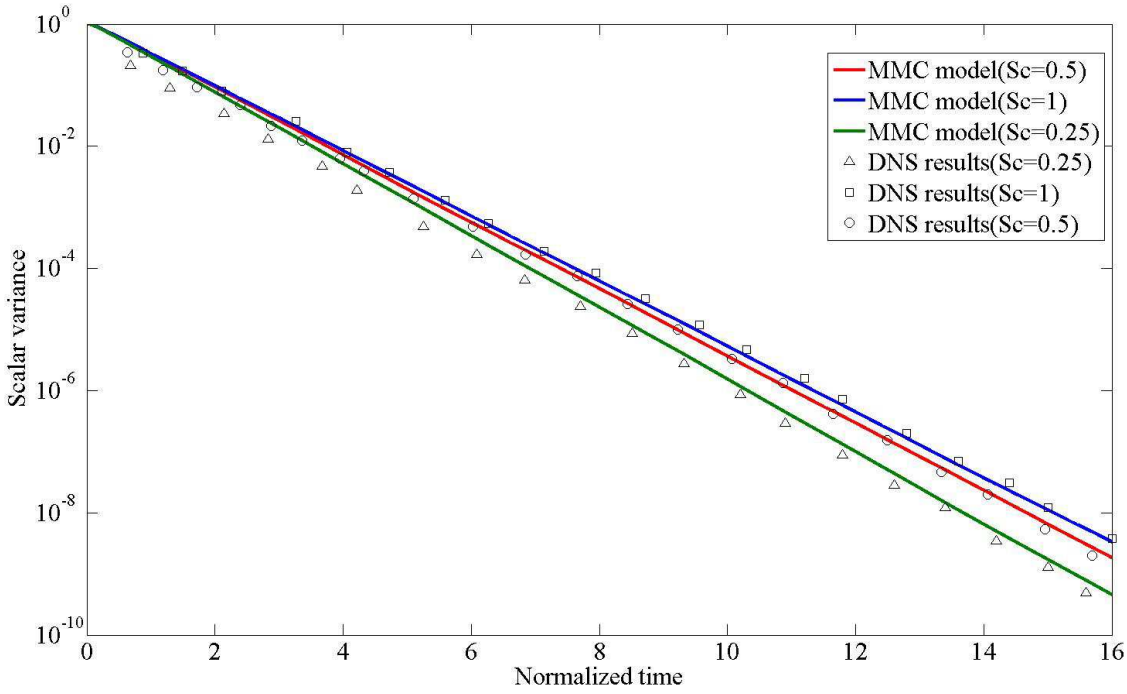

Figure 4.4. Scalar variances versus normalized time. Symbols denote DNS data of Yeung and Pope [17]; solid lines denote predictions by the MMC model with one reference variable.

A reasonable match between the MMC predicted decay rate and the DNS data of Yeung and Pope [17] for the first scalar ($Sc_1 = 1$) is obtained by setting $\Lambda = 0.1$, which is close the value of 1/8 used by Wandel and Klimenko [91] for a reacting but non-differentially diffusing case.

To match the decay rate of the second scalar we found that the best match was obtained with $C = 1.24$. Importantly the same set of model parameters are used for the two simulations and the model correctly predicts increasing scalar variance decay with decreasing Schmidt number.

C. A MMC model for predicting differential decay of scalar variance with controlled rate of decorrelation (two reference variable method)

In this section, we present a second MMC model which is capable of predicting both the differential scalar variance decay rates (as was the first model) and the rate of decorrelation of those differentially diffusing scalars. The first objective is handled with the side stepping method described in the preceding section. The second objective, to predict

the loss of correlation, is a much more difficult task. We propose a model with two independent reference variables, ζ_I and ζ_{II}, which are related to two independent Ornstein-Uhlenbeck processes, ξ_I and ξ_{II}, modelled according to equation (4.29). We set the major dissipation time scales as $\theta_I = \theta_{II}$. The reference variables are define as functions of ξ_I and ξ_{II}:

$$\zeta_I = \xi_I \tag{4.37a}$$

$$\zeta_{II} = f(\xi_I, \xi_{II}) \tag{4.37b}$$

Mixing occurs by localizing Y_I^* in ζ_I-space and Y_{II}^* in ζ_{II}-space and the function f therefore determines the rate of decorrelation of ζ_I and ζ_{II} and subsequently the decorrelation rate of Y_I^* and Y_{II}^*. A simple linear function is used here

$$\zeta_{II} = f(\xi_I, \xi_{II}) = a\xi_I + b\xi_{II} \tag{4.38}$$

where $a = \exp(-\mu t)$ and $b = \sqrt{1-a^2}$. The parameter μ is called the decorrelation parameter; a value of $\mu = 0$ corresponds to complete correlation of ζ_I and ζ_{II} at all times, while $\mu > 0$ results in an increasing rate of decorrelation. Note that if we set $\mu = 0$ the two-reference variable model is equivalent to the previous one-reference variable model.

The model works as follows. The Ornstein-Uhlenbeck processes ξ_I and ξ_{II} are advanced by a time increment dt at which point scalar Y_I^* is localised in ζ_I-space and mixed. At that point ξ_I and ξ_{II} are advanced by a further time increment $dt_s = r_s dt$ at which point scalar Y_{II}^* is localised in ζ_{II}-space and mixed. As described for the one reference variable model, that second time increment is a temporary side step and after mixing of scalar Y_{II}^* both ξ_I and ξ_{II} are returned to their values prior to the side step. As before, the side step parameter r_s is modelled according to equation (4.36).

The MMC model developed above is once again validated against the DNS data of Yeung and Pope [17] that was described in the previous section. In this section we also demonstrate correct scaling with Reynolds number by comparison with the DNS of Yeung and Luo [18] who looked at differentially diffusing scalar pairs ($Sc_I = 1$ and $Sc_{II} = 0.25$) over

a range of Taylor Reynolds numbers $\mathrm{Re}_\lambda = 38$, 70 and 90. Unless otherwise noted, the discussion below refers to the DNS of Yeung and Pope [17] with $\mathrm{Re}_\lambda = 38$. As before the MMC simulations are performed using 10,000 Pope particles and a numerical time step of 0.1 s.

Figure.4.5 shows the scalar variances versus normalized time for two scalars with $Sc_I = 1$ and $Sc_{II} = 0.25$. As for the one reference variable model the best results are found by setting $\Lambda = 0.1$ and $C = 1.24$. Note that this simulation covers a longer time duration than does the previous result shown in Figure 4.4, but the inset in Figure 4.5 shows the initial period for which DNS data are available.

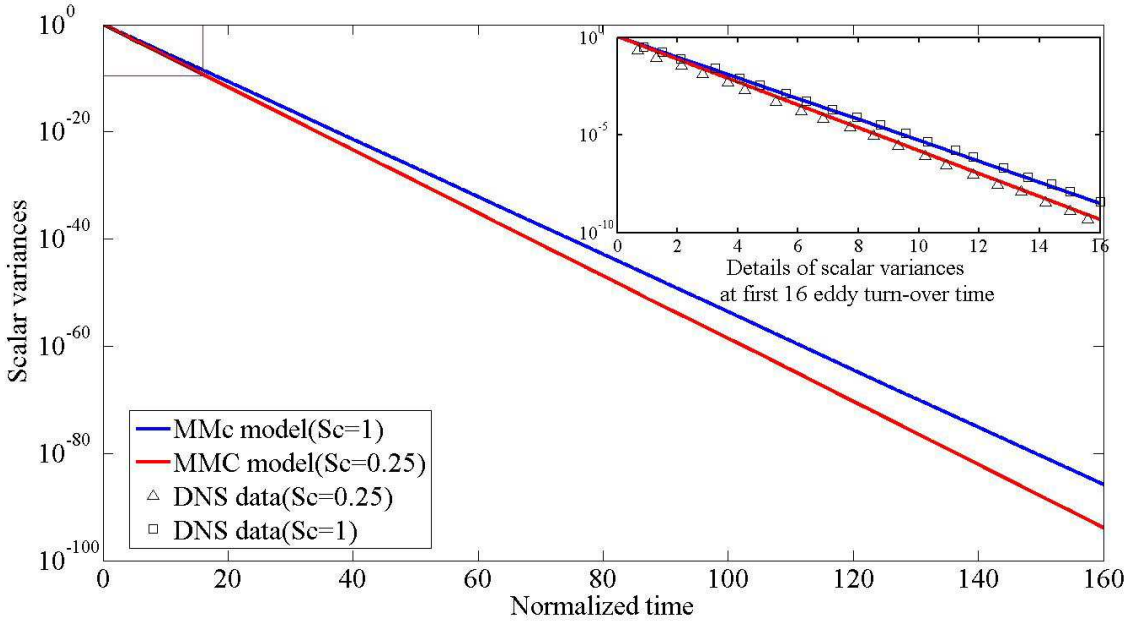

Figure 4.5. Scalar variances versus normalised time. Symbols denote DNS data of Yeung and Pope [17]; solid lines denote predictions by the MMC model with two reference variables.

We now analyse the scalar decorrelation. Figure 4.6 shows a scatter plot of Y_{II}^* versus Y_I^* for two scalars with $Sc_I = 1$ and $Sc_{II} = 0.25$ at 80 eddy turn-over times.

This result is for a simulation with the decorrelation parameter set to $\mu = 5\times10^{-5}$. Initially the two scalars are fully correlated and collapse to the red dashed line which has a slope of unity. Over time the scalars become decorrelated due to the action of differential diffusion as represented by the scatter data and the solid green mean line with a slope

less than one. A more quantitative perspective of the decorrelation is found in Figures 4.7 ,4.8 and 4.9. Figure 4.7 shows DNS data and model results for the correlation coefficient $\rho_{I,II}$ that is defined in equation (4.6) for two scalar pairs ($Sc_I = 1$, $Sc_{II} = 0.25$) and ($Sc_I = 1$, $Sc_{II} = 0.5$). Modelling is performed for five different values of μ. As expected $\mu = 0$ results in full correlation at all times. As previously mentioned the two reference variable model with $\mu = 0$ is equivalent to the one reference variable model. In this situation, although that model can accurately predict the differential decay of scalar variance, the scalars remain fully correlated which is counter to physical expectations. As μ is increased, the rate of decorrelation also increases.

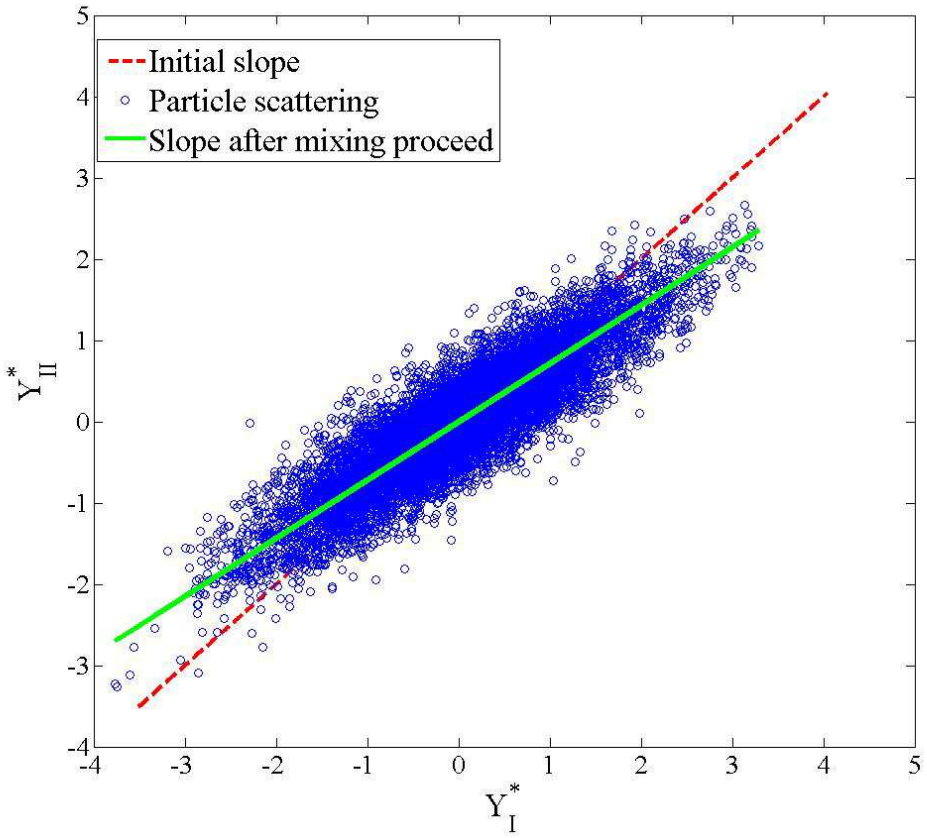

Figure 4.6. Particle scatter plot of Y^*_{II} versus Y^*_I at normalized time $t^* = 80$.

The best results for this particular flow are obtained by setting $\mu = 5\times10^{-5}$ for ($Sc_I = 1$, $Sc_{II} = 0.25$) and $\mu = 1.4\times10^{-5}$ for ($Sc_I = 1$, $Sc_{II} = 0.5$) while $\mu = 5\times10^{-6}$ yields excessively slow rate of decorrelation and $\mu = 5\times10^{-4}$ gives a decorrelation time that is an order of magnitude smaller than the DNS decorrelation time. Figure 4.8 illustrates the evolution of

the cross-correlation coefficient $\rho_{I,II}$ for two scalars with ($Sc_I = 1$, $Sc_{II} = 0.25$) at three different Reynolds numbers ($\mathrm{Re}_\lambda = 38, 70$ and 90) . Here the model results are compared with the DNS of Yeung and Luo [18] who reported scalar decorrelation rates for three different Reynolds numbers (but not the scalar variance decay rates). An appropriate agreement with DNS results for $\mathrm{Re}_\lambda = 38, 70$ and 90 are achieved by setting $\mu = 2.2\times10^{-5}$, 3×10^{-5} and 5×10^{-5}, respectively . It should be noted that in high Re simulations the initial value of the cross-correlation coefficient of two reference variables ζ_I and ζ_{II}, which is denoted by $\rho^{\zeta}{}_{I,II}$ and defined similarly to $\rho_{I,II}$ in equation (4.6), is slightly reduced in order to account for the initial adjustment of the correlation coefficients between two scalars ($Sc_I = 1$, $Sc_{II} = 0.25$) in the DNS [18]. From this simulation data, the decay rate of the scalar correlation coefficients can be scaled as $\mu \sim \mathrm{Re}^{-0.5}$ which is close to the $\rho^{-1}\,\mathrm{d}\rho/\mathrm{dt} \sim \mathrm{Re}^{-0.3}$ scaling suggested by Fox [65].

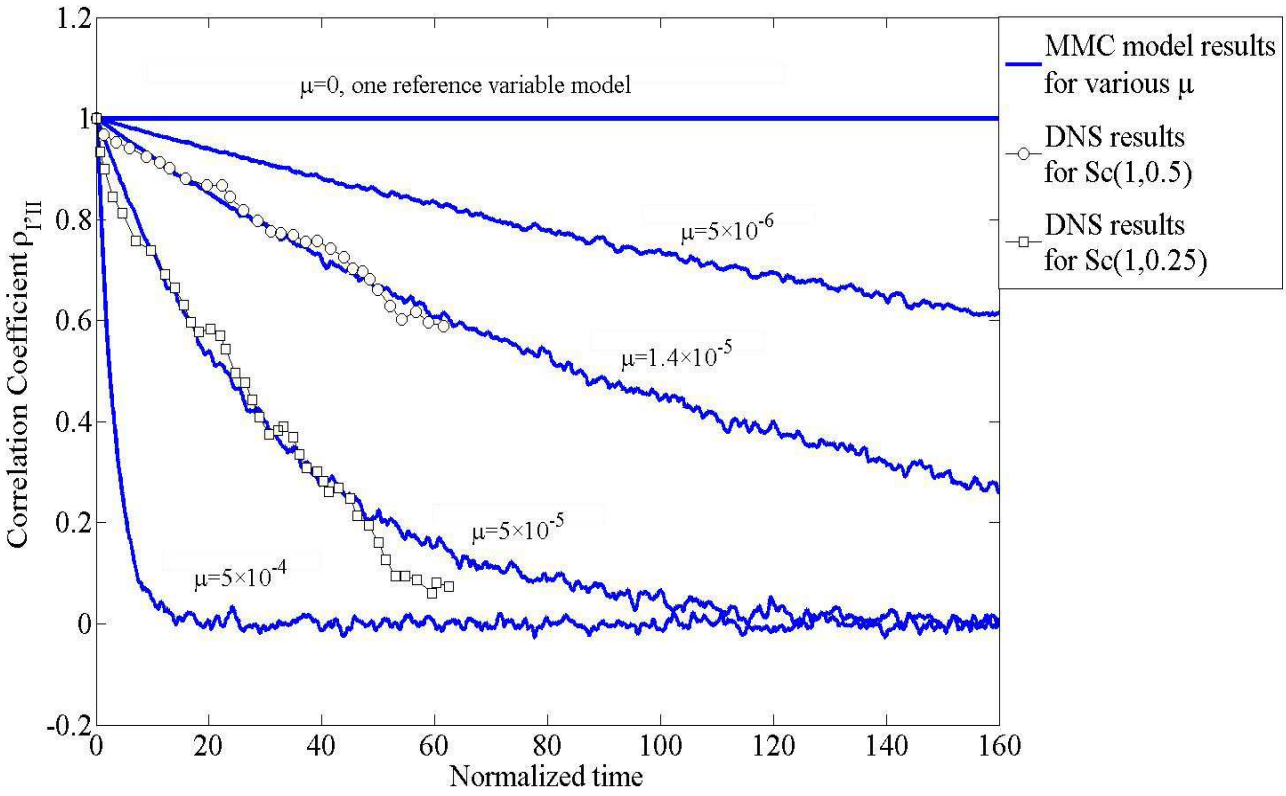

Figure 4.7. Evolution of the cross-correlation coefficient $\rho_{I,II}$ for different values of μ. Symbols denotes DNS data of Yeung and Pope [17]; blue solid lines denote predictions by the MMC model with two reference variables

It is clear from the results that the model correctly predicts a reduced rate of scalar decorrelation with increasing Reynolds number; which of course is indicative of the fact that differential diffusion is weaker at higher Reynolds number.

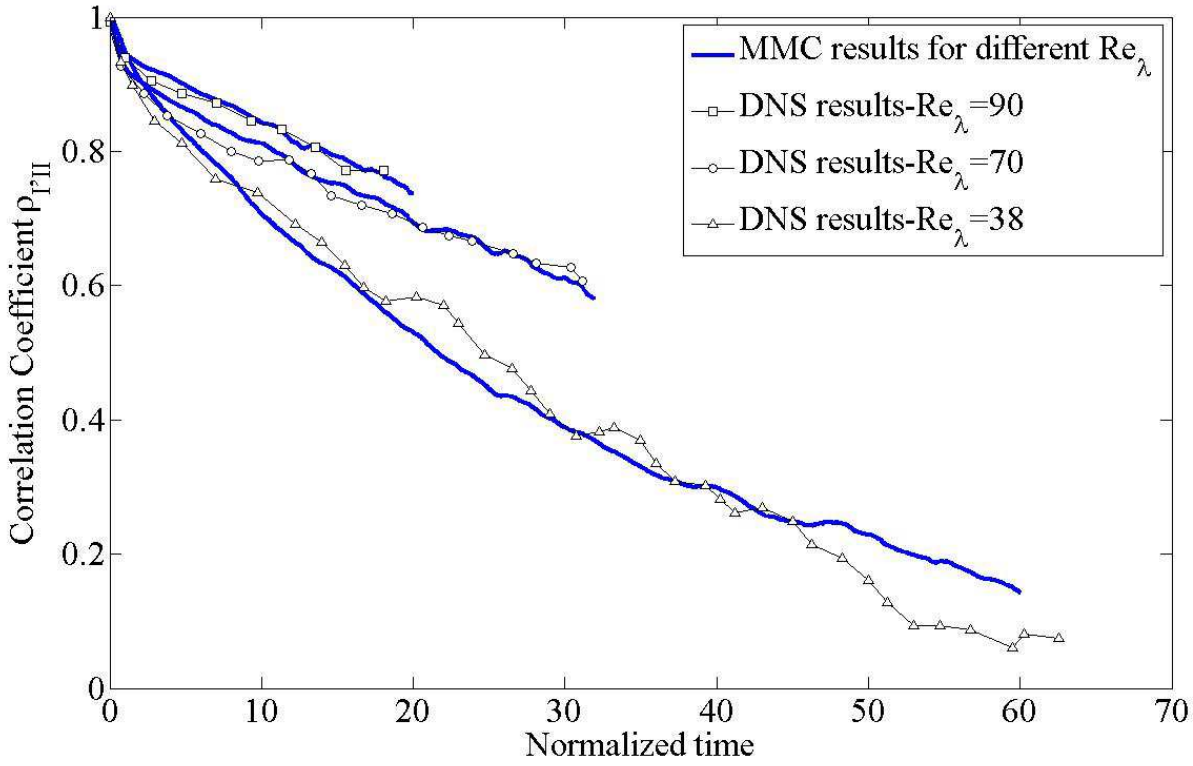

Figure 4.8. Evolution of the cross-correlation coefficient $\rho_{I,II}$ between two scalars ($Sc_I = 1$, $Sc_{II} = 0.25$) for three different Reynolds numbers . Symbols denote DNS data of Yeung and Luo [18] while solid lines denote predictions by the MMC model with two reference variables.

It is worthwhile to note the mechanism by which decorrelation of Y_I^* and Y_{II}^* is achieved in the model. The principles of MMC allow us to enforce the desirable decorelation rate on the simulated scalars without altering scalar values during mixing or adding any false source terms that can compromise the conservative properties of the model. . The scalars simply follow the decorrelation properties directly enforced on the reference variables ζ_I and ζ_{II}. The model directly controls $\rho^{\zeta}{}_{I,II}$, the cross-correlation coefficient between two reference variables ζ_I and ζ_{II} .

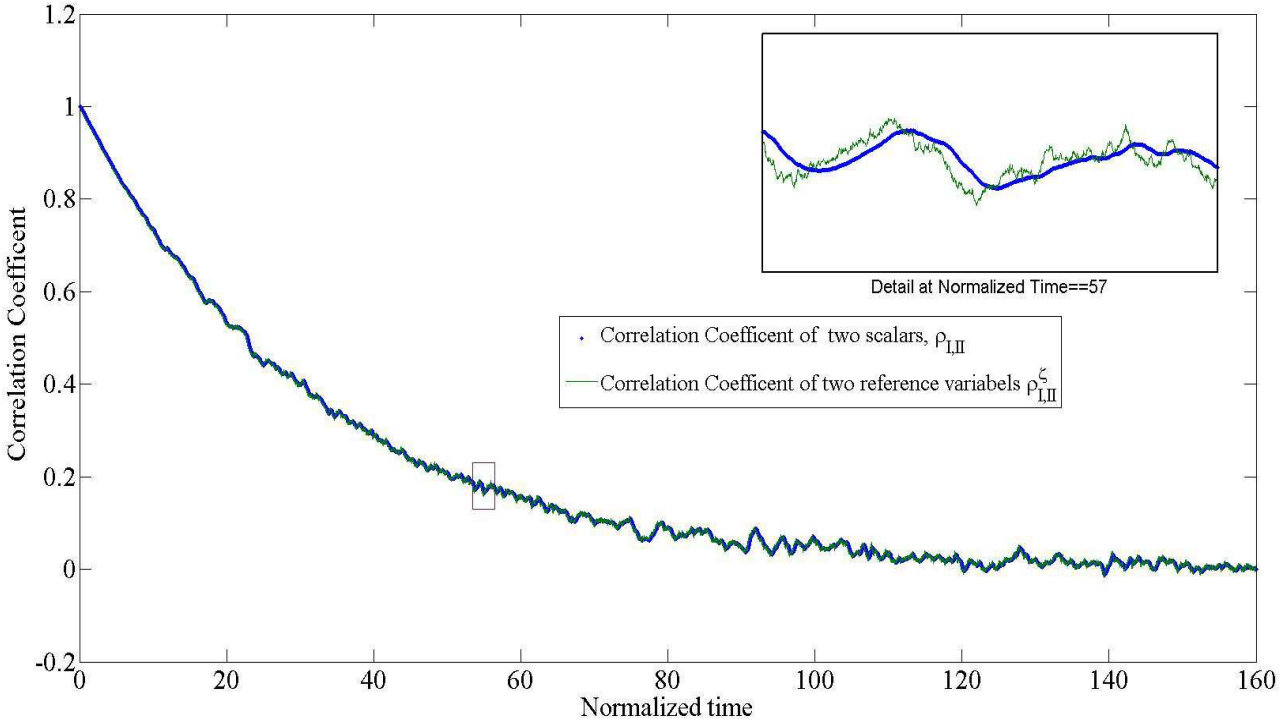

Figure 4.9. Evolution of the cross-correlation coefficients $\rho_{I,II}$ and $\rho^{\zeta}{}_{I,II}$ versus normalized time.

Figure 4.9 shows the evolution of both cross-correlation coefficients against normalized time for the case ($Sc_I = 1$, $Sc_{II} = 0.25$) with $\mu = 5\times10^{-5}$. The two values are closely aligned but as the inset figure taken at 57 eddy turn-over times shows $\rho^{\zeta}{}_{I,II}$ does have some scattering around $\rho_{I,II}$.

IV. Conclusion

The current work focuses on spatially homogeneous effects of differential diffusion and on their modelling within the MMC framework. First, the effects of differential diffusion are evaluated theoretically and in comparison with published experimental and DNS data. The dissipation time ratio is found to be proportional to $\mathrm{Re}^{-1/2}$. Second, the standard MMC model is modified to emulate the effects of differential diffusion.

The MMC mixing model is used to account for two important differential diffusion effects by using the reference variable concept. The difference in variance decay rates of two scalars with different diffusivities, which is the primary effect that is desired in practical simulations of differential diffusion, is modelled by using MMC with one reference variable. The concept of side-stepping which leads to an increase in the mixing window is discussed and

shown to be a practical and effective approach for modelling differential decay rates without need for a second reference variable. In this one reference variable MMC model the key parameter for controlling the difference in scalar decay rates have been linked to the ratio of the physical dissipation time scales. The second model, MMC with two reference variables, illustrates MMC's capability of modelling the more refined process of scalar decorrelation due to differential diffusion, while at the same time continued to accurately predict the difference in variance decay rates. By enforcing the appropriate correlation rates on two stochastically independent reference variables, the required decorrelation characteristics are automatically enforced by MMC on the simulated scalars. This is done without compromising integrity and universality of the mixing operator. The models are validated against DNS data for joint mixing of two scalars and the level of agreement is very good. In line with the theoretical developments, the models are also found to correctly predict the Reynolds numbers dependence of differential diffusion.

Future work will focus on the application of the new models for inhomogeneous shear flows.

Acknowledgments

This research is supported by the Australian Research Council under grant number DP120102294.

References

[1]J. Y. Chen and W. C. Chang,"Modeling Differential Diffusion Effects in Turbulent Nonreacting/Reacting Jets with Stochastic Mixing Models", Combustion Science and Technology **133** (4-6), 343-375 (1998).

[2]S. B. Pope,"PDF methods for turbulent reactive flows", Progress in Energy and Combustion Science **11** (2), 119-192 (1985).

[3]D. C. Haworth,"Progress in probability density function methods for turbulent reacting flows", Progress in Energy and Combustion Science **36** (2), 168-259 (2010).

[4]J. Janicka, W. Kolbe and W. Kollmann, in *Journal of Non-Equilibrium Thermodynamics* (1979), Vol. 4, pp. 47.

[5]C. Dopazo and E. E. O'Brien,"An approach to the autoignition of a turbulent mixture", Acta Astronautica **1** (9–10), 1239-1266 (1974).

[6]R. O. Fox,"The Lagrangian spectral relaxation model for differential diffusion in homogeneous turbulence", Physics of Fluids **11** (6), 1550 (1999).

[7]R. McDermott and S. B. Pope,"A particle formulation for treating differential diffusion in filtered density function methods", Journal of Computational Physics **226** (1), 947-993 (2007).

[8]E. S. Richardson and J. H. Chen,"Application of PDF mixing models to premixed flames with differential diffusion", Combustion and Flame **159** (7), 2398-2414 (2012).

[9]S. Subramaniam and S. B. Pope,"A mixing model for turbulent reactive flows based on Euclidean minimum spanning trees", Combustion and Flame **115** (4), 487-514 (1998).

[10]A. Kronenburg and R. W. Bilger,"Modelling of differential diffusion effects in nonpremixed nonreacting turbulent flow", Physics of Fluids **9** (5), 1435 (1997).

[11]A. Kronenburg and R. W. Bilger,"Modelling Differential Diffusion in Nonpremixed Reacting Turbulent Flow: Application to Turbulent Jet Flames", Combustion Science and Technology **166** (1), 175-194 (2001).

[12]N. S. A. Smith, in *1999 Australian symposium on combustion and sixth australian flame days* (University of Newcastle,Australia, 1999), pp. 61-65.

[13]A. Y. Klimenko and R. W. Bilger,"Conditional moment closure for turbulent combustion", Progress in Energy and Combustion Science **25** (6), 595-687 (1999).

[14]N. Peters,"Laminar diffusion flamelet models in non-premixed turbulent combustion", Progress in Energy and Combustion Science **10** (3), 319-339 (1984).

[15]V. R. Kuznetsov and V. A. Sabel'nikov, *Turbulence and Combustion*. (Hemisphere Publishing Corporation 1990).

[16]H. Pitsch and N. Peters,"A Consistent Flamelet Formulation for Non-Premixed Combustion Considering Differential Diffusion Effects", Combustion and Flame **114** (1–2), 26-40 (1998).

[17]H. Pitsch,"Unsteady flamelet modeling of differential diffusion in turbulent jet diffusion flames", Combustion and Flame **123** (3), 358-374 (2000).

[18]A. R. Kerstein,"Linear-eddy modelling of turbulent transport. Part 3. Mixing and differential molecular diffusion in round jets", Journal of Fluid Mechanics **216**, 411-435 (1990).

[19]M. Ulitsky, T. Vaithianathan and L. R. Collins,"A spectral study of differential diffusion of passive scalars in isotropic turbulence", Journal of Fluid Mechanics **460** (2002).

[20]R. W. Bilger,"Reaction rates in diffusion flames", Combustion and Flame **30** (0), 277-284 (1977).

[21]W. Bilger and R. W. Dibble,"Differential Molecular Diffusion Effects in Turbulent Mixing", Combustion Science and Technology **28** (3-4), 161-172 (1982).

[22]A. R. Kerstein, M. A. Cremer and P. A. McMurtry,"Scaling properties of differential molecular diffusion effects in turbulence", Physics of Fluids **7** (8), 1999 (1995).

[23]P. K. Yeung and S. B. Pope,"Differential diffusion of passive scalars in isotropic turbulence", Physics of Fluids A: Fluid Dynamics **5** (10), 2467-2478 (1993).

[24]P. K. Yeung,"Multi-scalar triadic interactions in differential diffusion with and without mean scalar gradients", Journal of Fluid Mechanics **321**, 235-278 (1996).

[25]P. K. Yeung, M. C. Sykes and P. Vedula,"Direct numerical simulation of differential diffusion with Schmidt numbers up to 4.0", Physics of Fluids **12** (6), 1601 (2000).

[26]P. K. Yeung and B. Luo, in *Proceedings of the 10th Symposium on Turbulent Shear Flows* (University Park, PA, 1995), pp. 31–37.

[27]F. A. Jaberi, R. S. Miller, F. Mashayek and P. Givi,"Differential Diffusion in Binary Scalar Mixing and Reaction", Combustion and Flame **109** (4), 561-577 (1997).

[28]V. Nilsen and G. Kosály,"Differentially diffusing scalars in turbulence", Physics of Fluids **9** (11), 3386 (1997).

[29]V. Nilsen and G. Kosály,"Differential diffusion in turbulent reacting flows", Combustion and Flame **117** (3), 493-513 (1999).

[30]M. C. Drake, R. W. Pitz and M. Lapp,"Laser Measurements on Nonpremixed & Air Flames for Assessment of Turbulent Combustion Models", AIAA Journal **24** (6), 905-917 (1986).

[31]M. C. Drake, M. Lapp, C. M. Penney, S. Warshaw and B. W. Gerhold,"Measurements of temperature and concentration fluctuations in turbulent diffusion flames using pulsed raman spectroscopy", Symposium (International) on Combustion **18** (1), 1521-1531 (1981).

[32]A. R. Masri, R. W. Dibble and R. S. Barlow,"Chemical kinetic effects in nonpremixed flames of H2/CO2 fuel", Combustion and Flame **91** (3–4), 285-309 (1992).

[33]L. L. Smith, R. W. Dibble, L. Talbot, R. S. Barlow and C. D. Carter,"Laser Raman scattering measurements of differential molecular diffusion in nonreacting turbulent jets of H2/CO2 mixing with air", Physics of Fluids **7** (6), 1455 (1995).

[34]R. Dibble and M. Long,"Investigation of differential diffusion in turbulent jet flows using planar laser Rayleigh scattering", Combustion and Flame **143** (4), 644-649 (2005).

[35]L. L. Smith, R. W. Dibble, L. Talbot, R. S. Barlow and C. D. Carter,"Laser Raman scattering measurements of differential molecular diffusion in turbulent nonpremixed jet flames of H2CO2 fuel", Combustion and Flame **100** (1–2), 153-160 (1995).

[36]V. Bergmann, W. Meier, D. Wolff and W. Stricker,"Application of spontaneous Raman and Rayleigh scattering and 2D LIF for the characterization of a turbulent CH4/H2/N2 jet diffusion flame", Appl Phys B **66** (4), 489-502 (1998).

[37]A. Y. Klimenko and S. B. Pope,"The modeling of turbulent reactive flows based on multiple mapping conditioning", Physics of Fluids **15** (7), 1907 (2003).

[38]M. J. Cleary and A. Y. Klimenko, in *Turbulent Combustion Modeling: Advances, New Trends and Perspectives*, edited by T.Echekki and E.Mastorakos (Springer Netherlands, 2011).

[39]A. Kronenburg and M. J. Cleary,"Multiple mapping conditioning for flames with partial premixing", Combustion and Flame **155** (1–2), 215-231 (2008).

[40]S. B. Pope,"A Model for Turbulent Mixing based on Shadow-Position Conditioning", Physics of Fluids (2013(in press)).

[41]A. N. Kolmogorov,"The Local Structure of Turbulence in Incompressible Viscous Fluid for Very Large Reynolds Numbers", Proceedings: Mathematical and Physical Sciences **434** (1890), 9-13 (1991).

[42]A.M.Oboukov,"Structure of the temperature field in a turbulent flow.", Izv. Akad. Nauk. SSSR, Geogr. i Geofiz **13**, 58-69 (1949).

[43]S. Corrsin,"Erratum: On the Spectrum of Isotropic Temperature Fluctuations in an Isotropic Turbulence", Journal of Applied Physics **22** (10), 1292-1292 (1951).

[44]G. K. Batchelor,"Small-scale variation of convected quantities like temperature in turbulent fluid Part 1. General discussion and the case of small conductivity", Journal of Fluid Mechanics **5** (01), 113-133 (1959).

[45]S. B. Pope, *Turbulent Flows*. (Cambridge University Press, 2000).

[46]P. A. Durbin and B. Pettersson-Reif, *Statistical theory and modeling for turbulent flows*. (Wiley, 2011).

[47]A. Y. Klimenko and M. J. Cleary,"Convergence to a Model in Sparse-Lagrangian FDF Simulations", Flow, Turbulence and Combustion **85** (3-4), 567-591 (2010).

[48]R. L. Curl,"Dispersed phase mixing: I. Theory and effects in simple reactors", AIChE Journal **9** (2), 175-181 (1963).

[49]M. J. Cleary and A. Y. Klimenko,"A detailed quantitative analysis of sparse-Lagrangian filtered density function simulations in constant and variable density reacting jet flows", Physics of Fluids **23** (11), 115102 (2011).

[50]A. Klimenko,"Matching conditional moments in PDF modelling of nonpremixed combustion", Combustion and Flame **143** (4), 369-385 (2005).

[51]A. Y. Klimenko,"On simulating scalar transport by mixing between Lagrangian particles", Physics of Fluids **19** (3), 031702 (2007).

[52]A. P. Wandel and A. Y. Klimenko,"Testing multiple mapping conditioning mixing for Monte Carlo probability density function simulations", Physics of Fluids **17** (12), - (2005).

Chapter 5 - Conclusion

The focus of this thesis is developing the Multiple Mapping Conditioning (MMC) method to incorporate differential diffusion effects. Following this objective, this study developed in two main parts.

In the first part, the theory of model has been developed. For further understanding of differential diffusion concept, its overview and several related numerical, experimental and model-development studies are reviewed. Moreover, the spectral view of turbulent motion based on eddy cascade hypothesis is discussed and developed for two cases of high and low Schmidt number. Then this spectral study has been continued for turbulent mixing of two differentially diffusing scalars Y_I and Y_{II} for two cases $Sc_{II} < Sc_I \leq 1$ and $Sc_{II} > Sc_I > 1$. The energy and variance spectrum of these scalars are considered for theoretical analysis of above-mentioned cases while the ratio of scalar dissipation timescales, τ_I / τ_{II}, is addressed to quantify differential diffusion effects. The Reynolds and Schmidt number scaling of this differential diffusion quantity are derived and compared with previous suggested results. This relation between differential diffusion and physical flow properties, characterised by Reynolds and Schmidt number, is used into the second part of the thesis to characterised the side stepping model parameter, r_s.

In the second part of this study, theoretical and methodological developments to standard MMC model have been implemented to deploy them to variants of MMC incorporating differential diffusion.

Two important differential diffusion effects are considered:

i. The difference in variance decay rates of two differentially diffusive scalars, which is the primary effect that needs to be emulated in practical simulations

ii. Scalar decorrelation, which is a more refined effect of differential diffusion

Both of the differential diffusion effects listed above are satisfied by two MMC models are presented in this research: a *one reference variable model* and a *two-reference variable model.*

In the first method, one reference variable model, the mixing of two scalars Y_I and Y_{II}, while $Sc_{II} < Sc_I < 1$, is localised based on a single reference variable which is modelled by

an Ornstein-Uhlenbeck stochastic processes. Modelling differential decay rate of two scalars is proposed by discussing the minor and major dissipation time scales in MMC and side-stepping approach. Essentially, in this approach mixing of more diffusive scalar is increased by increasing the available modelled time for its mixing to take place. The side step model parameter, r_s, controls the correct difference in decay rates while remaining linked to physical properties of flow.

The second model of MMC with two reference variables, can accurately predict both differential diffusion effects at the same time. Two stochastically independent reference variables that are related with a linear function were used to localise mixing of each scalar. Enforcing the appropriate correlation rates on two independent reference variables automatically results in the required decorrelation characteristics of two simulated differentially diffusive scalars. The model decorrelation parameter, μ, is set to obtain the desired results. Difference of scalar decay rate is also predicted by the same approach used in one reference variable model.

Both models are implemented numerically and validated against DNS data [17] , [18] with very good level of agreements.

For future work, it is suggested that these MMC models be applied to scalars with high Schmidt number as the theoretical part for this case is also developed in this study. More numerical resolution would be required for simulation of this case as scalar fluctuations dissipate at Batchelor's scale, which is smaller than Kolmogorov's scale.

Further interesting future work would be to generalise the new methodology for inhomogeneous, reacting flows and to apply the model to a practical hydrogen containing flame. The coupled influences of differential diffusion and chemical reaction would be more complex. This complexity is the challenging part of the above suggested development.

Bibliography

[1] A. International Energy, *World Energy Outlook 2015*: France: International Energy Agency, 2015.

[2] "WADEM Climate Change Position Statement," *Prehospital and Disaster Medicine,* vol. 32, pp. 351-351, 2017.

[3] S. McAllister, J.-Y. Chen, and A. C. Fernandez-Pello, *Fundamentals of Combustion Processes*. New York, NY: Springer New York, New York, NY, 2011.

[4] P. Nikolaidis and A. Poullikkas, "A comparative overview of hydrogen production processes," *Renewable and Sustainable Energy Reviews,* vol. 67, pp. 597-611, 2017/01/01/ 2017.

[5] T. da Silva Veras, T. S. Mozer, D. da Costa Rubim Messeder dos Santos, and A. da Silva César, "Hydrogen: Trends, production and characterization of the main process worldwide," *International Journal of Hydrogen Energy,* vol. 42, pp. 2018-2033, 2017/01/26/ 2017.

[6] Y. Bicer and I. Dincer, "Life cycle evaluation of hydrogen and other potential fuels for aircrafts," *International Journal of Hydrogen Energy,* vol. 42, pp. 10722-10738, 2017/04/20/ 2017.

[7] A. Demirbas, "Future hydrogen economy and policy," *Energy Sources, Part B: Economics, Planning, and Policy,* vol. 12, pp. 172-181, 2017/02/01 2017.

[8] N. Muradov, "Low to near-zero CO2 production of hydrogen from fossil fuels: Status and perspectives," *International Journal of Hydrogen Energy,* vol. 42, pp. 14058-14088, 2017/05/18/ 2017.

[9] S. Z. Baykara, "Hydrogen: A brief overview on its sources, production and environmental impact," *International Journal of Hydrogen Energy,* vol. 43, pp. 10605-10614, 2018/06/07/ 2018.

[10] P. A. Libby and F. A. Williams, *Turbulent Reacting Flows*: Berlin, Heidelberg : Springer Berlin Heidelberg, 1980.

[11] N. Peters, "Laminar diffusion flamelet models in non-premixed turbulent combustion," *Progress in Energy and Combustion Science,* vol. 10, pp. 319-339, 1984.

[12] N. Peters, *Turbulent Combustion*: Cambridge University Press, 2000.

[13] A. Y. Klimenko and R. W. Bilger, "Conditional moment closure for turbulent combustion," *Progress in Energy and Combustion Science,* vol. 25, pp. 595-687, 1999.

[14] S. B. Pope, "PDF methods for turbulent reactive flows," *Progress in Energy and Combustion Science,* vol. 11, pp. 119-192, 1985.

[15] S. B. Pope, *Turbulent Flows*: Cambridge University Press, 2000.

[16] A. Y. Klimenko and S. B. Pope, "The modeling of turbulent reactive flows based on multiple mapping conditioning," *Physics of Fluids,* vol. 15, p. 1907, 2003.

[17] P. K. Yeung and S. B. Pope, "Differential diffusion of passive scalars in isotropic turbulence," *Physics of Fluids A: Fluid Dynamics,* vol. 5, pp. 2467-2478, 1993.

[18] P. K. Yeung and B. Luo, "Simulation and modeling of differential diffusion in homogeneous turbulence," presented at the Proceedings of the 10th Symposium on Turbulent Shear Flows, University Park, PA, 1995.

[19] "Weather prediction by numerical process. By Lewis F. Richardson. Cambridge (University Press), 1922. 4°. Pp. xii + 236. 30s.net," vol. 48, ed. Bracknell, 1922, pp. 282-284.

[20] A. N. Kolmogorov, "A refinement of previous hypotheses concerning the local structure of turbulence in a viscous incompressible fluid at high Reynolds number," *J. Fluid Mech.,* vol. 13, pp. 82-85, 1962.

[21] A.M.Oboukov, "Structure of the temperature field in a turbulent flow.," *Izv. Akad. Nauk. SSSR, Geogr. i Geofiz,* vol. 13, pp. 58-69, 1949.

[22] S. Corrsin, "On the Spectrum of Isotropic Temperature Fluctuations in an Isotropic Turbulence," *Journal of Applied Physics,* vol. 22, pp. 469-473, 1951.

[23] G. K. Batchelor, "Small-scale variation of convected quantities like temperature in turbulent fluid Part 1. General discussion and the case of small conductivity," *Journal of Fluid Mechanics,* vol. 5, pp. 113-133, 1959.

[24] R. M. Kerr, "Velocity, scalar and transfer spectra in numerical turbulence," *Journal of Fluid Mechanics,* vol. 211, pp. 309-332, 1990.
[25] F. A. Williams, *Combustion Theory: The Fundamental Theory of Chemically Reacting Flow Systems*: Perseus Books Group, 1985.
[26] T. Poinsot and D. Veynante, *Theoretical and Numerical Combustion, 2/E*: R.T. Edwards, 2005.
[27] N. Peters, "Local Quenching Due to Flame Stretch and Non-Premixed Turbulent Combustion," *Combustion Science and Technology,* vol. 30, pp. 1-17, 1983.
[28] V. Kuznetsov, "Influence of turbulence on the formation of high nonequilibrium concentrations of atoms and free radicals in diffusion flames," *Fluid Dynamics,* vol. 17, pp. 815-820, 1982.
[29] A. Y. Klimenko, "Multicomponent diffusion of various admixtures in turbulent flow," *Fluid Dynamics,* vol. 25, pp. 327-334, 1990/05/01 1990.
[30] R. W. Bilger, "Conditional moment closure for turbulent reacting flow," *Physics of Fluids A: Fluid Dynamics,* vol. 5, pp. 436-444, 1993.
[31] C. Dopazo, "Probability density function approach for a turbulent axisymmetric heated jet. Centerline evolution," *Physics of Fluids,* vol. 18, p. 397, 1975.
[32] S. B. Pope, "The probability approach to the modelling of turbulent reacting flows," *Combustion and Flame,* vol. 27, pp. 299-312, 1976.
[33] A. Y. Klimenko and M. J. Cleary, "Convergence to a Model in Sparse-Lagrangian FDF Simulations," *Flow, Turbulence and Combustion,* vol. 85, pp. 567-591, 2010.
[34] V. Raman, H. Pitsch, and R. Fox, "Hybrid large-eddy simulation/Lagrangian filtered-density-function approach for simulating turbulent combustion," *Combustion and Flame,* vol. 143, pp. 56-78, 2005.
[35] S. B. Pope, "Computations of turbulent combustion: Progress and challenges," *Symposium (International) on Combustion,* vol. 23, pp. 591-612, 1991.
[36] F. Gao and E. E. O'Brien, "A large-eddy simulation scheme for turbulent reacting flows," *Physics of Fluids A: Fluid Dynamics,* vol. 5, pp. 1282-1284, 1993.
[37] T. Drozda, M. Sheikhi, C. Madnia, and P. Givi, "Developments in Formulation and Application of the Filtered Density Function," *An International Journal published in association with ERCOFTAC,* vol. 78, pp. 35-67, 2007.
[38] S. Subramaniam and S. B. Pope, "A mixing model for turbulent reactive flows based on Euclidean minimum spanning trees," *Combustion and Flame,* vol. 115, pp. 487-514, 1998.
[39] J. Janicka, W. Kolbe, and W. Kollmann, "Closure of the Transport Equation for the Probability Density Funcfion of Turbulent Scalar Fields," in *Journal of Non-Equilibrium Thermodynamics* vol. 4, ed, 1979, p. 47.
[40] R. L. Curl, "Dispersed phase mixing: I. Theory and effects in simple reactors," *AIChE Journal,* vol. 9, pp. 175-181, 1963.
[41] H. Chen, S. Chen, and R. H. Kraichnan, "Probability distribution of a stochastically advected scalar field," *Physical Review Letters,* vol. 63, pp. 2657-2660, 1989.
[42] S. B. Pope, "A model for turbulent mixing based on shadow-position conditioning," *Physics of Fluids (1994-present),* vol. 25, p. 110803, 2013.
[43] U. Maas and S. B. Pope, "Simplifying chemical kinetics: Intrinsic low-dimensional manifolds in composition space," *Combustion and Flame,* vol. 88, pp. 239-264, 1992.
[44] M. J. Cleary and A. Y. Klimenko, "Multiple Mapping Conditioning: A New Modelling Framework for Turbulent Combustion," in *Turbulent Combustion Modeling: Advances, New Trends and Perspectives*, T.Echekki and E.Mastorakos, Eds., ed: Springer Netherlands, 2011.
[45] A. Klimenko, "Matching conditional moments in PDF modelling of nonpremixed combustion," *Combustion and Flame,* vol. 143, pp. 369-385, 2005.
[46] M. J. Cleary and A. Y. Klimenko, "A detailed quantitative analysis of sparse-Lagrangian filtered density function simulations in constant and variable density reacting jet flows," *Physics of Fluids,* vol. 23, p. 115102, 2011.
[47] R. W. Bilger, "Reaction rates in diffusion flames," *Combustion and Flame,* vol. 30, pp. 277-284, 1977.

[48] H. Tsuji and I. Yamaoka, "Structure analysis of counterflow diffusion flames in the forward stagnation region of a porous cylinder," *Symposium (International) on Combustion,* vol. 13, pp. 723-731, 1971.
[49] W. Bilger and R. W. Dibble, "Differential Molecular Diffusion Effects in Turbulent Mixing," *Combustion Science and Technology,* vol. 28, pp. 161-172, 1982.
[50] P. K. Yeung, "Multi-scalar triadic interactions in differential diffusion with and without mean scalar gradients," *Journal of Fluid Mechanics,* vol. 321, pp. 235-278, 1996.
[51] V. Nilsen and G. Kosály, "Differentially diffusing scalars in turbulence," *Physics of Fluids,* vol. 9, p. 3386, 1997.
[52] A. R. Kerstein, M. A. Cremer, and P. A. McMurtry, "Scaling properties of differential molecular diffusion effects in turbulence," *Physics of Fluids,* vol. 7, p. 1999, 1995.
[53] F. A. Jaberi, R. S. Miller, F. Mashayek, and P. Givi, "Differential Diffusion in Binary Scalar Mixing and Reaction," *Combustion and Flame,* vol. 109, pp. 561-577, 1997.
[54] N. S. A. Smith, "Differential diffusion of passive scalars in homogeneous turbulence:implications for combustion modeling," presented at the 1999 Australian symposium on combustion and sixth Australian flame days, University of Newcastle,Australia, 1999.
[55] V. Nilsen and G. Kosály, "Differential diffusion in turbulent reacting flows," *Combustion and Flame,* vol. 117, pp. 493-513, 1999.
[56] P. K. Yeung, M. C. Sykes, and P. Vedula, "Direct numerical simulation of differential diffusion with Schmidt numbers up to 4.0," *Physics of Fluids,* vol. 12, p. 1601, 2000.
[57] P. K. Yeung, "Correlations and conditional statistics in differential diffusion: Scalars with uniform mean gradients," *Physics of Fluids,* vol. 10, p. 2621, 1998.
[58] M. C. Drake, M. Lapp, C. M. Penney, S. Warshaw, and B. W. Gerhold, "Measurements of temperature and concentration fluctuations in turbulent diffusion flames using pulsed raman spectroscopy," *Symposium (International) on Combustion,* vol. 18, pp. 1521-1531, 1981.
[59] M. C. Drake, R. W. Pitz, and M. Lapp, "Laser Measurements on Nonpremixed & Air Flames for Assessment of Turbulent Combustion Models," *AIAA Journal,* vol. 24, pp. 905-917, 1986/06/01 1986.
[60] A. R. Masri, R. W. Dibble, and R. S. Barlow, "Chemical kinetic effects in nonpremixed flames of H2/CO2 fuel," *Combustion and Flame,* vol. 91, pp. 285-309, 1992.
[61] L. L. Smith, R. W. Dibble, L. Talbot, R. S. Barlow, and C. D. Carter, "Laser Raman scattering measurements of differential molecular diffusion in nonreacting turbulent jets of H2/CO2 mixing with air," *Physics of Fluids,* vol. 7, p. 1455, 1995.
[62] C. J. B. a. L. K. Su, "Experimental investigation of differential diffusion in turbulent mixing using planar imaging measurements," *44th Aerospace Sciences Meeting and Exhibit, 9-12 January 2006, Reno, Nevada,* 2006.
[63] R. Dibble and M. Long, "Investigation of differential diffusion in turbulent jet flows using planar laser Rayleigh scattering," *Combustion and Flame,* vol. 143, pp. 644-649, 2005.
[64] T. M. Lavertu, L. Mydlarski, and S. J. Gaskin, "Differential diffusion of high-Schmidt-number passive scalars in a turbulent jet," *Journal of Fluid Mechanics,* vol. 612, 2008.
[65] R. O. Fox, "The Lagrangian spectral relaxation model for differential diffusion in homogeneous turbulence," *Physics of Fluids,* vol. 11, p. 1550, 1999.
[66] C. J. Brownell and L. K. Su, "Planar laser imaging of differential molecular diffusion in gas-phase turbulent jets," *Physics of Fluids,* vol. 20, 2008.
[67] L. L. Smith, R. W. Dibble, L. Talbot, R. S. Barlow, and C. D. Carter, "Laser Raman scattering measurements of differential molecular diffusion in turbulent nonpremixed jet flames of H2CO2 fuel," *Combustion and Flame,* vol. 100, pp. 153-160, 1995.
[68] V. Bergmann, W. Meier, D. Wolff, and W. Stricker, "Application of spontaneous Raman and Rayleigh scattering and 2D LIF for the characterization of a turbulent CH4/H2/N2 jet diffusion flame," *Applied Physics B,* vol. 66, pp. 489-502, 1998/04/01 1998.
[69] W. Meier, S. Prucker, M. H. Cao, and W. Stricker, "Characterization of Turbulent hytVAir Jet Diffusion Flames by Single-Pulse Spontaneous Raman Scattering," *Combustion Science and Technology,* vol. 118, pp. 293-312, 1996/10/01 1996.
[70] A. R. Kerstein, "Linear-eddy modelling of turbulent transport. Part 3. Mixing and differential molecular diffusion in round jets," *Journal of Fluid Mechanics,* vol. 216, pp. 411-435, 1990.

[71] A. Kronenburg and R. W. Bilger, "Modelling of differential diffusion effects in nonpremixed nonreacting turbulent flow," *Physics of Fluids,* vol. 9, p. 1435, 1997.
[72] A. Kronenburg and R. W. Bilger, "Modelling Differential Diffusion in Nonpremixed Reacting Turbulent Flow: Application to Turbulent Jet Flames," *Combustion Science and Technology,* vol. 166, pp. 175-194, 2001.
[73] V. R. Kuznetsov and V. A. Sabel'nikov, *Turbulence and Combustion*: Hemisphere Publishing Corporation 1990.
[74] H. Pitsch and N. Peters, "A Consistent Flamelet Formulation for Non-Premixed Combustion Considering Differential Diffusion Effects," *Combustion and Flame,* vol. 114, pp. 26-40, 1998.
[75] H. Pitsch, "Unsteady flamelet modeling of differential diffusion in turbulent jet diffusion flames," *Combustion and Flame,* vol. 123, pp. 358-374, 2000.
[76] S. Sannan and A. R. Kerstein, "Differential Molecular Diffusion in a Hydrogen-Rich Jet," *Energy Procedia,* vol. 86, pp. 304-314, 2016.
[77] S. Sannan and A. R. Kerstein, "Numerical Simulation of Differential Molecular Diffusion Effects in a Hydrogen-rich Turbulent Jet Using LEM3D," *Energy Procedia,* vol. 51, pp. 253-258, 2014.
[78] J. Y. Chen and W. C. Chang, "Modeling Differential Diffusion Effects in Turbulent Nonreacting/Reacting Jets with Stochastic Mixing Models," *Combustion Science and Technology,* vol. 133, pp. 343-375, 1998.
[79] C. Dopazo and E. E. O'Brien, "An approach to the autoignition of a turbulent mixture," *Acta Astronautica,* vol. 1, pp. 1239-1266, 1974.
[80] R. McDermott and S. B. Pope, "A particle formulation for treating differential diffusion in filtered density function methods," *Journal of Computational Physics,* vol. 226, pp. 947-993, 2007.
[81] E. S. Richardson and J. H. Chen, "Application of PDF mixing models to premixed flames with differential diffusion," *Combustion and Flame,* vol. 159, pp. 2398-2414, 2012.
[82] D. C. Haworth, "Progress in probability density function methods for turbulent reacting flows," *Progress in Energy and Combustion Science,* vol. 36, pp. 168-259, 2010.
[83] M. Ulitsky, T. Vaithianathan, and L. R. Collins, "A spectral study of differential diffusion of passive scalars in isotropic turbulence," *Journal of Fluid Mechanics,* vol. 460, 2002.
[84] A. Kronenburg and M. J. Cleary, "Multiple mapping conditioning for flames with partial premixing," *Combustion and Flame,* vol. 155, pp. 215-231, 2008.
[85] S. B. Pope, "A Model for Turbulent Mixing based on Shadow-Position Conditioning," *Physics of Fluids,* 2013(in press).
[86] A. N. Kolmogorov, "The Local Structure of Turbulence in Incompressible Viscous Fluid for Very Large Reynolds Numbers," *Proceedings: Mathematical and Physical Sciences,* vol. 434, pp. 9-13, 1991.
[87] S. Corrsin, "Erratum: On the Spectrum of Isotropic Temperature Fluctuations in an Isotropic Turbulence," *Journal of Applied Physics,* vol. 22, pp. 1292-1292, 1951.
[88] P. A. Durbin and B. Pettersson-Reif, *Statistical theory and modeling for turbulent flows*: Wiley, 2011.
[89] A. Y. Klimenko, "On simulating scalar transport by mixing between Lagrangian particles," *Physics of Fluids,* vol. 19, p. 031702, 2007.
[90] J. Janicka, W. Kolbe, and W. Kollmann, "Closure of the Transport Equation for the Probability Density Funcfion of Turbulent Scalar Fields," *Journal of Non-Equilibrium Thermodynamics,* vol. 4, p. 47, 1979.
[91] A. P. Wandel and A. Y. Klimenko, "Testing multiple mapping conditioning mixing for Monte Carlo probability density function simulations," *Physics of Fluids,* vol. 17, pp. -, 2005.